First-order one-electron properties in the integral-direct coupled cluster singles and doubles model

Asger Halkier, Henrik Koch, Ove Christiansen, and Poul Jørgensen
Department of Chemistry, University of Aarhus, DK-8000 Aarhus C, Denmark

Trygve Helgaker
Department of Chemistry, University of Oslo, P.O. Box 1033 Blindern, N-0315 Oslo, Norway

(Received 25 September 1996; accepted 11 April 1997)

An integral-direct implementation of first-order one-electron properties in the coupled cluster singles and doubles (CCSD) model is presented. The implementation increases the range of applicability of CCSD first-order one-electron property calculations significantly compared to nondirect approaches. As an application a thorough basis set investigation is performed on five diatomic molecules at the Hartree–Fock and CCSD levels for the molecular electric dipole moment, the molecular electric quadrupole moment, and the electric field gradient at the nuclei. In general, basis sets of polarized triple-zeta quality are the smallest to be recommended, and the convergence towards the basis set limit is faster at the Hartree–Fock level than at the CCSD level. Among the properties considered, the electric dipole moment is the easiest to converge. The electric dipole and especially the electric quadrupole moment require diffuse functions for high accuracy. With standard basis sets, it is not possible to calculate electric field gradients consistently within three thousandths of an atomic unit of the basis set limit—for this purpose, elaborate nonstandard basis sets are required. The electric field gradients at the nuclei in HCN and the electric dipole moment of the furan molecule are calculated at the CCSD level employing up to 417 basis functions, further demonstrating the large-scale applicability of the implementation. © *1997 American Institute of Physics.* [S0021-9606(97)02927-9]

I. INTRODUCTION

During the last decade, the coupled cluster singles and doubles (CCSD) model has gained popularity as an accurate method for describing the dynamical correlation effects in molecular systems. Several implementations of the CCSD model have been presented[1–5] and a variety of molecular properties have successfully been calculated at this level.[6–20] However, the disk-space requirements for the storage of integrals has imposed severe limitations on the size of the molecular systems that can be studied using ''conventional'' implementations (the limit being around 300 basis functions). To solve this problem, Koch *et al.* presented an integral-direct implementation of the CCSD ground-state energy and calculations with up to 548 basis functions have been reported.[18,19] The integral-direct scheme has recently been extended to the calculation of excitation energies, and CCSD excitation energy calculations with up to 432 basis functions have been reported.[20]

In the CCSD model, however, there is a significant difference between obtaining the ground-state energy and first-order one-electron properties. In order to obtain the ground-state energy we only need to solve equations for obtaining the coupled cluster (CC) reference wave function. A first-order one-electron property is an expectation value of an one-electron operator. Because of the nonvariational nature of the CCSD model, the calculation of expectation values is *not* a trivial extension of ground-state energy calculations. One additional set of CC equations need to be solved before the expectation value can be evaluated. The solution of these equations in an integral-direct fashion is presented in the first part of this paper.

The expressions for first-order one-electron properties are special cases of the general expressions for first-order energy derivatives,[21] and the implementation presented below therefore constitutes a first step towards an integral-direct implementation of CCSD gradients, required for efficient geometry optimizations. Furthermore, the left and right linear transformations of the CCSD Jacobian described in this paper and in Ref. 20, respectively, are the basic building blocks for the calculation of *all* other response properties.

We here consider calculations of the molecular electric dipole moment (DPM), the molecular electric quadrupole moment (QPM), and the electric field gradient at the nuclei (EFG). These properties are all important quantities characterizing the charge distribution of a molecular electronic system. However, the EFGs are particularly interesting from the point of view of a computational chemist. First, the accurate calculation of the electric field gradient q at a light nucleus, combined with the experimental determination of the quadrupole coupling constant eqQ/h, constitutes the most accurate method for obtaining the nuclear quadrupole moment Q of the light nuclei.[22,23] Conversely, calculated EFGs combined with a nuclear quadrupole moment give predicted values of the quadrupole coupling constants, which can be compared with experimental results from microwave and NMR experiments. Second, the EFG depends as r^{-3} on the radial distance r from the nucleus in question and therefore puts severe demands on the basis sets, making the accurate calcu-

lation of EFGs a very difficult task. Indeed, we need both a good description of the valence region to describe the chemical bonding correct and a good description of the core and inner valence regions in order to get the dominant contributions to the EFG correct.

As a first application demonstrating the possibilities the integral-direct implementation has made possible, we perform a thorough basis set investigation of DPM, QPM, and EFG. Such an investigation requires calculations with basis sets of polarized quintuple-zeta quality which result in several calculations with more than 350 basis functions, which can only be carried out using the integral-direct implementation.

Sundholm *et al.*[24] have carried out numerical Hartree–Fock calculations of molecular electric multipole moments and EFGs for several diatomics including BF, CO, HF, N_2, and NO^+. Therefore, by performing systematic Hartree–Fock and CCSD calculations of the lowest multipole moments and EFGs for these systems, we should be able to obtain valuable information about the performance of the different basis sets for these properties both at the uncorrelated and correlated levels. Among the standard basis sets investigated here, the Dunning series cc-pCVXZ and aug-cc-pCVXZ,[25–29] $X = D,T,Q,5$, provide the best results for the EFGs, as may be expected since these sets are designed to correlate core as well as valence electrons.

To demonstrate the performance and applicability of the integral-direct CCSD algorithm compared with other theoretical approaches, we present results for the EFGs in hydrogen cyanide and compare with other theoretical studies. The use of the most elaborate and accurate basis sets is made possible only because of the implementation of the integral-direct scheme, allowing us to obtain results close to the CCSD basis set limit. Correlation effects beyond CCSD are shown to be important, demonstrating the need for extending the model to include the effects of triple excitations.

As a final application we have calculated the DPM of the furan molecule (C_4H_4O) to demonstrate the possibilities of the present algorithm in comparison with experimental studies. It has not been possible to determine the sign of the DPM of furan by experiments alone, but the absolute value is well known from experiments. The present calculations establish the sign of the DPM of furan and agree well with the experimentally determined absolute value of this.

In Sec. II, we review the theory for the calculation of CCSD first-order one-electron properties and present the integral-direct implementation. The results of a basis set investigation of 29 standard basis sets are given in Sec. III. In Sec. IV, we present the results of the large-scale calculations of the EFGs in HCN and compare with other theoretical results. In Sec. V the results of the calculations of the DPM of furan is presented. Finally, in Sec. VI, we give our concluding remarks.

II. INTEGRAL-DIRECT CCSD FIRST-ORDER ONE-ELECTRON PROPERTIES

A. The CCSD model

Consider a closed-shell system described by the Hamiltonian H. The single-reference CCSD wave function is given by the exponential *ansatz*

$$|\mathrm{CC}\rangle = \exp(T)|\mathrm{HF}\rangle, \tag{1}$$

where the cluster operator contains contributions from single and double excitations only

$$T = T_1 + T_2, \tag{2}$$

where

$$T_1 = \sum_{ai} t_i^a E_{ai}, \tag{3}$$

$$T_2 = \sum_{(ai)\geqslant(bj)} t_{ij}^{ab} E_{ai} E_{bj}. \tag{4}$$

Orbital indices a,b,c,d,e,f and i,j,k,l,m,n refer to unoccupied and occupied molecular orbitals (MOs) in the Hartree–Fock state, respectively, whereas indices p,q,r,s,t,u are general MO indices. In a shorthand notation, the cluster operator is written in the form

$$T = \sum_{\mu=1,2} t_\mu \tau_\mu, \tag{5}$$

where τ_μ are the excitation operators and t_μ the associated cluster amplitudes.

The CC energy is obtained by projecting the CC Schrödinger equation against the Hartree–Fock reference state

$$E_{\mathrm{CC}} = \langle \mathrm{HF}|H \exp(T)|\mathrm{HF}\rangle \tag{6}$$

and the cluster amplitudes are determined by projecting the CC Schrödinger equation against the excitation manifold of the Hartree–Fock reference state

$$\langle \mu|\exp(-T)H \exp(T)|\mathrm{HF}\rangle = 0. \tag{7}$$

Here,

$$\langle \mu| = \langle \mathrm{HF}|\tau_\mu^+ \tag{8}$$

and the Hamiltonian in the second quantization formalism is given by

$$H = \sum_{pq} h_{pq} E_{pq} + \frac{1}{2} \sum_{pqrs} g_{pqrs} e_{pqrs}. \tag{9}$$

B. Theory of CCSD first-order properties

The detailed derivation of the CCSD gradient, and hence first-order one-electron property expressions, is well documented elsewhere.[30–32] First-order one-electron properties are conveniently expressed as

$$\langle A \rangle = \sum_{pq} a_{pq} D_{pq}, \tag{10}$$

where a_{pq} are the integrals over the operator associated with the property A and we have introduced the relaxed CC one-electron density

$$D_{pq}=\left\{\langle \mathrm{HF}|+\sum_{\mu}\overline{t_{\mu}}\langle\mu|\exp(-T)\right\}E_{pq}|\mathrm{CC}\rangle + \sum_{ai}\overline{\kappa_{ai}}\langle \mathrm{HF}|[E_{ai}^{-},E_{pq}]|\mathrm{HF}\rangle, \tag{11}$$

where

$$E_{ai}^{-}=E_{ai}-E_{ia}. \tag{12}$$

In Eq. (11), the $\overline{t_{\mu}}$ parameters are the zero-order Lagrange multipliers for the cluster amplitudes and $\overline{\kappa_{ai}}$ the similar orbital-rotation multipliers. Neglecting the orbital-relaxation term in Eq. (11), we obtain unrelaxed first-order one-electron properties. In this study, we work exclusively with the fully relaxed density in Eq. (11).

The cluster amplitudes were determined by solving Eq. (7), but before we can evaluate the one-electron density in Eq. (11), we need to determine the zero-order one-electron cluster amplitude Lagrange multipliers and orbital rotation Lagrange multipliers $\overline{t_{\mu}}$ and $\overline{\kappa_{ai}}$. These are obtained from the zero-order response equations

$$\sum_{\mu}\overline{t_{\mu}}\langle\mu|\exp(-T)[H,\tau_{\nu}]|\mathrm{CC}\rangle=-\langle \mathrm{HF}|[H,\tau_{\nu}]|\mathrm{CC}\rangle, \tag{13}$$

$$\sum_{bj}\overline{\kappa_{bj}}\langle \mathrm{HF}|[E_{bj}^{-},[E_{ai}^{-},H]]|\mathrm{HF}\rangle = -\left\{\langle \mathrm{HF}|+\sum_{\mu}\overline{t_{\mu}}\langle\mu|\exp(-T)\right\}[E_{ai}^{-},H]|\mathrm{CC}\rangle. \tag{14}$$

When solving large sets of linear equations such as Eqs. (13) and (14), iterative methods are mandatory. The most expensive step is the repeated transformation of trial vectors on the coefficient matrix (here the response matrix). Computationally, the transformation on the left-hand side of Eq. (13) is the most demanding of the two transformations required for the zero-order Lagrange multipliers. This particular transformation is therefore discussed in detail below. The transformation needed for solving Eq. (14) is identical to the one used for solving the Hartree–Fock response equations,[21] although the right-hand side of course is different. The evaluation of the comparatively inexpensive right-hand side of Eq. (14) is closely related to our gradient implementation, and will therefore be discussed in our forthcoming paper on integral-direct CCSD gradients.[33] The final evaluation of the first-order one-electron property expression Eq. (10) is trivial once the relaxed CC one-electron density D has been constructed. The construction of D emerges naturally in the context of the full gradient and will therefore be discussed in Ref. 33.

C. Linear transformation in cluster amplitude multiplier response equations

We now consider the linear transformation in Eq. (13) consisting of a left transformation of a trial vector ζ on the CCSD Jacobian

$$\rho_{\nu}=\sum_{\mu=1,2}\zeta_{\mu}\langle\mu|\exp(-T_2-T_1)[H,\tau_{\nu}]\times\exp(T_1+T_2)|\mathrm{HF}\rangle,\quad \nu=1,2. \tag{15}$$

Here, ζ_1,ζ_2 and ρ_1,ρ_2 are single- and double-excitation parts of the trial vectors and the transformed trial vectors, respectively. Introducing the T_1-similarity transformed Hamiltonian

$$\hat{H}=\exp(-T_1)H\ \exp(T_1) \tag{16}$$

we may write the transformed vectors as

$$\rho_{\nu}=\sum_{\mu=1,2}\zeta_{\mu}\langle\mu|\exp(-T_2)[\hat{H},\tau_{\nu}]\exp(T_2)|\mathrm{HF}\rangle,\quad \nu=1,2 \tag{17}$$

which can be expanded to yield

$$\rho_1=\sum_{\mu_1}\zeta_{\mu_1}\langle\mu_1|[\hat{H},\tau_1]+[[\hat{H},\tau_1],T_2]|\mathrm{HF}\rangle + \sum_{\mu_2}\zeta_{\mu_2}\langle\mu_2|[\hat{H},\tau_1]+[[\hat{H},\tau_1],T_2]|\mathrm{HF}\rangle, \tag{18}$$

$$\rho_2=\sum_{\mu_1}\zeta_{\mu_1}\langle\mu_1|[\hat{H},\tau_2]|\mathrm{HF}\rangle+\sum_{\mu_2}\zeta_{\mu_2}\langle\mu_2|[\hat{H},\tau_2] + [[\hat{H},\tau_2],T_2]|\mathrm{HF}\rangle. \tag{19}$$

Following Ref. 18, the T_1-similarity transformation in Eq. (16) leads to the modified Hamiltonian

$$\hat{H}=\hat{h}+\hat{g}=\sum_{pq}\hat{h}_{pq}E_{pq}+\tfrac{1}{2}\sum_{pqrs}\hat{g}_{pqrs}e_{pqrs} \tag{20}$$

whose integrals are given as

$$\hat{h}_{pq}=\sum_{\alpha\beta}h_{\alpha\beta}\Lambda^{p}_{\alpha p}\Lambda^{h}_{\beta q}, \tag{21}$$

$$\hat{g}_{pqrs}=\sum_{\alpha\beta\gamma\delta}g_{\alpha\beta\gamma\delta}\Lambda^{p}_{\alpha p}\Lambda^{h}_{\beta q}\Lambda^{p}_{\gamma r}\Lambda^{h}_{\delta s}. \tag{22}$$

Here, Λ^{p} and Λ^{h} are effective MO transformation matrices (particle and hole transformations, respectively) constructed from the singles amplitudes and the MO coefficients as described in Refs. 18–20. In Eqs. (21) and (22), we have also extended the orbital indices convention, reserving Greek letters for AO basis indices.

The benefit of working with the Hamiltonian in Eq. (16) is that the structure of the equations becomes simpler since the singles amplitudes are not referenced directly. The cost is that the usual eightfold permutational symmetry of the integrals is lost with only the particle-permutation symmetry of the two-electron integrals retained

$$\hat{g}_{pqrs}=\hat{g}_{rspq}. \tag{23}$$

We will use the following basis for the excitation manifold:

$$\langle\mu_1|=\langle \mathrm{HF}|E_{ia}\tfrac{1}{2}, \tag{24}$$

$$\langle\mu_2|=\langle \mathrm{HF}|(2E_{ia}E_{jb}+E_{ja}E_{ib})\tfrac{1}{6}(1+\delta_{ab}\delta_{ij})^{-1},$$

$$(ai)\geqslant(bj). \tag{25}$$

Together with the excited ket states $E_{ai}|\mathrm{HF}\rangle$ and $E_{ai}E_{bj}|\mathrm{HF}\rangle$ obtained using the excitation operators in Eqs. (3) and (4), these bra states constitute a biorthonormal basis. We have now presented the tools needed for evaluating Eqs. (18) and (19). Explicit expressions are given in the Appendix where, for completeness, we also give the expression for the right-hand side in Eq. (13). However, since this term is inexpensive and easily constructed, we do not discuss it further here. Note that, for the derivation in the Appendix, we have extended the restricted summation in the doubles operator, Eq. (4), to a full summation

$$T_2=\sum_{(ai)\geqslant(bj)} t_{ij}^{ab}E_{ai}E_{bj}=\tfrac{1}{2}\sum_{aibj} t_{ij}^{ab}(1+\delta_{ij}\delta_{ab})E_{ai}E_{bj} \tag{26}$$

and absorbed the diagonal factor in the doubles amplitudes

$$t_{ij}^{ab}(1+\delta_{ab}\delta_{ij})\rightarrow t_{ij}^{ab}. \tag{27}$$

D. Implementation

The idea underlying the integral-direct CCSD algorithm is the calculation of AO integrals in distributions, where all two-electron integrals with one fixed AO index δ are calculated simultaneously

$$I_{\alpha\beta,\gamma}^{\delta}=g_{\alpha\beta\gamma\delta}, \quad \alpha\geqslant\beta. \tag{28}$$

In practice, all distributions with indices δ belonging to the same shell and related by symmetry are calculated simultaneously and written to disk. Subsequently, these distributions are read back into memory—one by one—in a loop over all symmetry-related δ indices belonging to the shell in question.

An efficient implementation of Eqs. (A2)–(A8) and (A12)–(A19) in the integral-direct scheme is not trivial—disk and memory requirements, operation counts, and vectorization must all be taken into consideration. Clearly, the final implementation becomes a compromise between these requirements. As in the integral-direct algorithm for the right transformation of the Jacobian, we introduce both global and local intermediates.[20] The global intermediates are independent of the trial vectors—they are evaluated once and for all and then stored on disk for reuse. The local intermediates, on the other hand, depend on the trial vectors—they are recalculated in each iteration and kept in memory. The use of intermediates reduces the operation count but increases disk and memory requirements.

In the following, we shall consider the implementation of the computationally most demanding terms only—that is, the terms that scale as N^6. (Here, N denotes the total number of orbitals and we shall use V and O for the number of virtual and occupied orbitals, respectively, below.) We shall therefore not consider the implementation of the terms (A2)–(A6) and (A17)–(A19).

Consider the double excitation part of the transformed vector. Written as in Eq. (A10), this part requires 8 N^6 processes. The expressions in parenthesis in the A, C, and D terms are all independent of ζ_μ. They are already used as global intermediates in the excitation-energy code,[20] and are used globally here as well. The intermediates are read back into memory after the δ loop one at a time, contracted with the appropriate trial-vector amplitudes, and added to the transformed vector. The B term is similar to the B terms of Refs. 19 and 20 and is constructed as in Ref. 19. The E term is constructed using a local intermediate

$$M_{ijmn}=\sum_{cd}\zeta_{ij}^{cd}t_{mn}^{cd} \tag{29}$$

(requiring O^4 in memory) which is contracted with the integrals in MO basis outside the δ loop (the integrals $\hat{g}_{manb}$ are global intermediates as well).

In the single-excitation part of the transformed vector in Eq. (A1), there appears to be another eight N^6 processes. The last term in parenthesis in Eq. (A8) is similar to the B term in Eq. (A13) but with summation indices referring to hole indices rather than particle indices. Since the intermediate $\Omega_{\alpha\beta,kl}^{\mathrm{BF}}$ of Ref. 19 is used globally in the excitation-energy code,[20] we manipulate the last term in Eq. (A8) so as to utilize the same intermediate

$$\rho_{iG(\mathrm{last})}^{a}=-\sum_{dkl}\zeta_{kl}^{da}\sum_{\alpha\beta}\Lambda_{\alpha d}^{p}\Lambda_{\beta i}^{p}\Omega_{\alpha\beta,kl}^{\mathrm{BF}} \tag{30}$$

and note that we then obtain the last term of Eq. (A6) at no extra cost. The last term in Eq. (A7) is calculated using the local M intermediate in Eq. (29), which is contracted with the integral I_{jkl}^{δ} and finally scaled with the Λ^h matrix in the δ loop.

The remaining 6 N^6 processes can be calculated using four local intermediates inside the δ loop, requiring 3 N^6 processes. The four intermediates are

$$t_{dkj}^{\delta}=\sum_{f}t_{kj}^{df}\Lambda_{\delta f}^{h}, \tag{31}$$

$$Z_{eij}^{\delta}=\sum_{dk}\zeta_{ik}^{ed}t_{dkj}^{\delta}; \quad W_{eij}^{\delta}=\sum_{dk}\zeta_{ik}^{ed}t_{djk}^{\delta};$$

$$V_{eij}^{\delta}=\sum_{dk}\zeta_{ik}^{de}t_{djk}^{\delta}. \tag{32}$$

The final six computationally intensive terms may thus be written as

$$\rho^a_{i,\text{rem.int.terms}} = \sum_{lj\delta} (V^\delta_{alj} + Z^\delta_{alj})\hat{g}_{jli\delta} + \sum_{lj\delta} (W^\delta_{alj} - 2Z^\delta_{alj})\hat{g}_{ilj\delta} + \sum_{ej\delta} (2Z^\delta_{eij} - W^\delta_{eij})\hat{g}_{eaj\delta} - \sum_{ej\delta} (Z^\delta_{eij} + V^\delta_{eij})\hat{g}_{jae\delta}. \quad (33)$$

Since the present implementation uses the same global intermediates as the excitation-energy code, the disk requirements are the same. The memory requirements are, on the other hand, somewhat larger in the present transformation. The memory allocation is at its peak in the δ loop, where we need to hold in core the integral distribution ($1/2N^3$), a packed transformed vector ($1/2N^2O^2$), a packed cluster amplitude ($1/2V^2O^2$), and a squared (for better vectorization) trial vector (V^2O^2). These requirements should be compared with the memory requirement $1/2N^3 + 1/2N^2O^2 + V^2O^2$ of the energy and excitation-energy codes.[19,20] However, from the discussion above we note that instead of 16 N^6 processes in each iteration, we can get by with only eight and timings from the calculations below indicate that one iteration is slightly faster than one ground-state energy iteration. This implies that the total cost of obtaining CCSD first order one-electron properties is approximately twice that of obtaining the CCSD ground-state energy.

III. BASIS SET INVESTIGATION

A. Computational details

We shall here examine 29 commonly used basis sets, see Table I.[25–29,34–39] For each basis, we have listed the number of contracted functions for each angular momentum in the first-row atoms, as well as the total number of basis functions in calculations on the diatomics BF,.../HF, recalling that all diatomics containing two first-row atoms give rise to the same number of basis functions.

The operator representing DPM is

$$\mu_\alpha = \sum_B Q_B R_{B\alpha} - \sum_i r_{i\alpha}, \quad (34)$$

where the first summation is over nuclei with charges Q_B and position vectors R_B and the second is over the electrons with position vectors r_i. Here, and below, Greek letter subscripts represent Cartesian directions.

For QPM, we use the traceless moment as defined by Buckingham[40]

$$\Theta_{\alpha\beta} = \tfrac{1}{2}\sum_B Q_B(3R_{B\alpha}R_{B\beta} - \delta_{\alpha\beta}R_B^2) - \tfrac{1}{2}\sum_i (3r_{i\alpha}r_{i\beta} - \delta_{\alpha\beta}r_i^2). \quad (35)$$

The operator for the electric field gradient at nucleus A is given by

TABLE I. Name and total number of basis functions in calculations on BF, CO, N_2, NO^+/HF for the 29 investigated basis sets. Also given is the number of contracted functions in each shell ($s,p,\ldots$) on first row atoms. The numbers in the ANO names refer to the number of contracted $s,p,d,(f)$ functions on first row atoms (first) and hydrogen (last).

Basis set	# contracted functions s	p	d	f	g	i	# basis functions BF,.../HF
6-311G	4	3	-	-	-	-	26/16
6-311G**	4	3	1	-	-	-	36/24
6-311G(2*d*,2*p*)	5	4	2	-	-	-	54/36
6-311++G**	5	4	1	-	-	-	44/29
6-311++G(2*d*,2*p*)	5	4	2	-	-	-	54/37
DZP (Ahlrichs)	4	2	1	-	-	-	30/20
TZP (Ahlrichs)	6	3	1	-	-	-	40/26
TZ2P (Ahlrichs)	6	3	2	-	-	-	50/34
Sadlej	5	3	2	-	-	-	48/33
ANO 4321_321	4	3	2	1	-	-	60/44
ANO 5432_432	5	4	3	2	-	-	92/69
ANO 6543_543	6	5	4	3	-	-	124/94
ANO 7643_643	7	6	4	3	-	-	132/99
cc-pVDZ	3	2	1	-	-	-	28/19
cc-pVTZ	4	3	2	1	-	-	60/44
cc-pVQZ	5	4	3	2	1	-	110/85
cc-pV5Z	6	5	4	3	2	1	182/146
aug-cc-pVDZ	4	3	2	-	-	-	46/32
aug-cc-pVTZ	5	4	3	2	-	-	92/69
aug-cc-pVQZ	6	5	4	3	2	-	160/126
aug-cc-pV5Z	7	6	5	4	3	2	254/207
cc-pCVDZ	4	3	1	-	-	-	36/23
cc-pCVTZ	6	5	3	1	-	-	86/57
cc-pCVQZ	8	7	5	3	1	-	168/114
cc-pCV5Z	10	9	7	5	3	1	290/200
aug-cc-pCVDZ	5	4	2	-	-	-	54/32
aug-cc-pCVTZ	7	6	4	2	-	-	118/73
aug-cc-pCVQZ	9	8	6	4	2	-	218/139
aug-cc-pCV5Z	11	10	8	6	4	2	362/236

$$q_{\alpha\beta}(A) = \sum_{B\neq A} Q_B \frac{3R_{BA\alpha}R_{BA\beta} - \delta_{\alpha\beta}R_{BA}^2}{R_{BA}^5} - \sum_i \frac{3r_{iA\alpha}r_{iA\beta} - \delta_{\alpha\beta}r_{iA}^2}{r_{iA}^5}, \quad (36)$$

where the summations are over the remaining nuclei with position vectors R_{BA} relative to A and the electrons with position vectors r_{iA} relative to A.

Since DPM is linear in r_i, a good description of the outer valence regions is required for high accuracy. It is therefore important to include diffuse functions in the basis set. The same argument applies to QPM, for which the diffuse functions become even more important because of the quadratic dependence on the position vectors. The EFG, in contrast, requires a good description of the core region as well as the inner valence region because of the r_i^{-3} dependence. For this property inclusion of tight basis functions therefore becomes important.

For linear molecules, we have a single nontrivial component of the DPM. The QPM and EFG tensors are automatically diagonal with elements labeled as $|q_{33}| \geqslant |q_{22}| \geqslant |q_{11}|$. Since for linear molecules $q_{33} = -2q_{22} = -2q_{11}$,[40] we shall report only the 33-component below.

TABLE II. Calculated Hartree–Fock molecular electric dipole moments in atomic units. Numerical results from Ref. 24.

Basis set	BF	CO	HF	NO^+
6-311G	0.1694	0.1961	−0.9181	0.3227
6-311G**	0.3405	0.1060	−0.7945	0.2840
6-311G(2*d*,2*p*)	0.3312	0.1054	−0.7793	0.2551
6-311++G**	0.3193	0.1194	−0.8131	0.2735
6-311++G(2*d*,2*p*)	0.3312	0.1054	−0.7789	0.2551
DZP (Ahlrichs)	0.3695	0.1190	−0.7703	0.2969
TZP (Ahlrichs)	0.3291	0.1273	−0.8101	0.2672
TZ2P (Ahlrichs)	0.3368	0.1048	−0.7729	0.2545
Sadlej		0.1006	−0.7566	0.2499
ANO 4321_321	0.3546	0.0999	−0.7591	0.2544
ANO 5432_432	0.3469	0.1026	−0.7563	0.2558
ANO 6543_543	0.3424	0.1044	−0.7563	0.2539
ANO 7643_643	0.3427	0.1045	−0.7564	0.2540
cc-pVDZ	0.3472	0.0919	−0.7670	0.2836
cc-pVTZ	0.3485	0.0966	−0.7637	0.2586
cc-pVQZ	0.3412	0.1041	−0.7607	0.2556
cc-pV5Z	0.3418	0.1049	−0.7602	0.2540
aug-cc-pVDZ	0.3539	0.1020	−0.7597	0.2500
aug-cc-pVTZ	0.3434	0.1050	−0.7574	0.2530
aug-cc-pVQZ	0.3427	0.1043	−0.7563	0.2536
aug-cc-pV5Z	0.3428	0.1042	−0.7561	0.2537
cc-pCVDZ	0.3465	0.0916	−0.7676	0.2851
cc-pCVTZ	0.3442	0.1017	−0.7636	0.2611
cc-pCVQZ	0.3414	0.1044	−0.7607	0.2557
cc-pCV5Z	0.3418	0.1048	−0.7601	0.2540
aug-cc-pCVDZ	0.3532	0.1046	−0.7745	0.2514
aug-cc-pCVTZ	0.3420	0.1052	−0.7611	0.2535
aug-cc-pCVQZ	0.3427	0.1044	−0.7570	0.2537
aug-cc-pCV5Z	0.3428	0.1043	−0.7563	0.2537
Numerical result	0.3428	0.1042	−0.7561	0.2537

B. Hartree–Fock results

Since we wish to benchmark the performance of the different basis sets against the numerical Hartree–Fock results of Sundholm *et al.*,[24] we shall here use the geometries of Ref. 24: $R(\mathrm{BF})=2.386$ a.u., $R(\mathrm{CO})=2.132$ a.u., $R(\mathrm{HF})=1.7328$, $R(\mathrm{N_2})=2.068$ a.u., $R(\mathrm{NO^+})=2.0092$ a.u. All calculations are carried out in the center-of-mass coordinate system.

1. Dipole moment results

In Table II, the Hartree–Fock DPMs for the different basis sets are listed together with the numerical results.[24] Note that there is no Sadlej basis set for boron. It is gratifying to see that the elaborate aug-cc-pV5Z basis does reproduce the numerical results to four decimals places for all four molecules. In Fig. 1, the magnitudes of the deviation from the numerical results of the two series cc-pVXZ and aug-cc-pVXZ are given. A comparison of the results for the two series illustrates the importance of including diffuse functions in the basis when DPMs are calculated. We note that the convergence of the aug-cc-pVXZ series towards the basis set limit is an excellent one and clearly indicative of a hierarchical structure: The major part of the errors at the aug-cc-pVDZ level is gone at the aug-cc-pVTZ level, and, proceeding to the aug-cc-pVQZ level, the DPMs are for all practical purposes converged to the basis set limit.

Included in Fig. 1 are also the ANO results. The convergence of this series is also good although we do not fully reach the numerical results, being around 0.2 milliatomic units (mau) off. The aug-cc-pVXZ series may be used for obtaining the Hartree–Fock basis set limit results. However, since the number of contracted basis functions in the ANO sets is significantly smaller than in the aug-cc-pVXZ series, our results indicate that, in Hartree–Fock calculations, one can cover larger systems with the former sets practically with the accuracy of the latter.

We believe there are two reasons for the good performance of the comparatively small ANO basis sets: (1) The additional diffuse functions included in the Dunning sets upon augmentation are already part of the basic ANO primitive set, and (2) the ANO contraction coefficients are based on calculations on the neutral atom as well as on calculations on the cation and the anion. The calculation on the anion introduces a diffuse character in the basis, thereby making it well suited for accurate DPM calculations.

Comparing the core–valence and the valence Dunning sets, we find—as expected—that the core contributions to the DPMs are rather small, especially for the larger sets. Since the additional core functions make the calculations significantly more expensive, there appears to be no compelling reason for the use of the core–valence basis sets in DPM calculations on molecules containing first-row atoms only.

The Sadlej basis gives a very good result for HF, being in error by only 0.5 mau, but for CO and NO^+ the errors are around 4 mau. The accuracy fluctuates and—since we can only perform ''one shot'' calculations with this basis set—it is not recommended for high accuracy calculations.

The results for the three Ahlrichs sets reveal that these basis sets are too small for high-accuracy DPM calculations. The largest set (TZ2P) gives good results for CO and NO^+, but its performance—like that of the Sadlej set—fluctuates, with HF being 16.8 mau from the basis set limit.

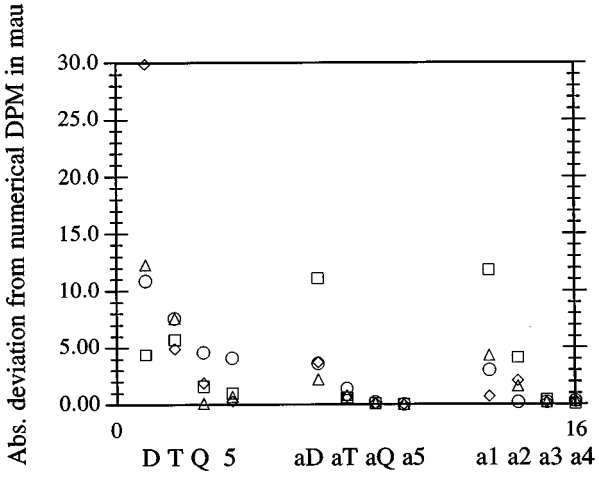

FIG. 1. The absolute value of the deviation from the numerical Hartree–Fock dipole moments (Ref. 24) in mau. D is short for cc-pVDZ and similarly aD stands for aug-cc-pVDZ an so on through the Dunning series. The ANO series are denoted *a*1 to *a*4 increasing in since with the number.

TABLE III. Calculated Hartree–Fock 33-component of traceless molecular electric quadrupole moment tensor in atomic units. Numerical results from Ref. 24.

Basis set	BF	CO	HF	NO^+	N_2
6-311G	−3.6048	−2.1497	1.6298	−0.2185	−1.7127
6-311G**	−3.2141	−1.6504	1.6565	0.3545	−1.1850
6-311G(2*d*,2*p*)	−3.1366	−1.5115	1.7454	0.5693	−0.9236
6-311++G**	−3.1732	−1.6699	1.7113	0.3525	−1.1554
6-311++(2*d*,2*p*)	−3.1366	−1.5115	1.7459	0.5693	−0.9236
DZP (Ahlrichs)	−3.2853	−1.6892	1.6627	0.3592	−1.2245
TZP (Ahlrichs)	−3.3246	−1.7521	1.7116	0.3181	−1.2436
TZ2P (Ahlrichs)	−3.1702	−1.5483	1.7188	0.5329	−0.9902
Sadlej		−1.5059	1.7448	0.5690	−0.9232
ANO 4321_321	−3.1518	−1.5676	1.7422	0.5371	−0.9495
ANO 5432_432	−3.1764	−1.5370	1.7317	0.5191	−0.9400
ANO 6543_543	−3.1555	−1.5347	1.7277	0.5185	−0.9408
ANO 7643_643	−3.1563	−1.5325	1.7296	0.5186	−0.9398
cc-pVDZ	−3.1327	−1.5608	1.6457	0.4155	−1.1335
cc-pVTZ	−3.1482	−1.5285	1.6912	0.5048	−1.0269
cc-pVQZ	−3.1563	−1.5328	1.7056	0.5171	−0.9820
cc-pV5Z	−3.1569	−1.5405	1.7183	0.5163	−0.9701
aug-cc-pVDZ	−3.0867	−1.5823	1.7344	0.5354	−0.9042
aug-cc-pVTZ	−3.1537	−1.5460	1.7348	0.5204	−0.9356
aug-cc-pVQZ	−3.1533	−1.5304	1.7348	0.5219	−0.9352
aug-cc-pV5Z	−3.1557	−1.5304	1.7327	0.5191	−0.9388
cc-pCVDZ	−3.1330	−1.5564	1.6472	0.4158	−1.1315
cc-pCVTZ	−3.1648	−1.5327	1.6890	0.5058	−1.0223
cc-pCVQZ	−3.1562	−1.5325	1.7056	0.5167	−0.9821
cc-pCV5Z	−3.1567	−1.5396	1.7184	0.5168	−0.9695
aug-cc-pCVDZ	−3.0833	−1.5281	1.7628	0.5364	−0.9039
aug-cc-pCVTZ	−3.1555	−1.5403	1.7450	0.5255	−0.9296
aug-cc-pCVQZ	−3.1529	−1.5296	1.7384	0.5225	−0.9345
aug-cc-pCV5Z	−3.1556	−1.5303	1.7332	0.5193	−0.9386
daug-cc-pVTZ	−3.1584	−1.5341	1.7382	0.5204	−0.9378
daug-cc-pVQZ	−3.1562	−1.5299	1.7339	0.5200	−0.9371
Numerical h.f.	−3.1562	−1.5300	1.7321	0.5191	−0.9400

The Pople basis sets occasionally give good results but are usually off by more than 10 mau and are therefore not suited for accurate DPM calculations.

2. Quadrupole moment results

The calculated Hartree–Fock QPMs are given in Table III, along with the numerical results.[24] As for DPMs, the aug-cc-pV5Z basis gives the most accurate results. However, even with this elaborate basis set, we are still not fully converged to the basis set limit. The maximum error relative to the numerical results is 1.2 mau and the mean of the absolute errors is 0.5 mau. In Fig. 2, the magnitude of the deviation from the numerical results is shown for the same three series of basis sets as in Fig. 1. A comparison of the two Dunning series in Fig. 2 demonstrates clearly the need for diffuse functions. The convergence in the aug-cc-pVXZ sequence is again good, although in a few isolated cases the error in the QPM is not reduced as we go to a larger basis set. However, the mean absolute deviations decreases steadily from aug-cc-pVDZ to aug-cc-pV5Z: 35.2 (aD), 5.4 (aT), 2.7 (aQ), and 0.5 ($a5$) mau.

The performance of the ANO series is virtually as good as that of the aug-cc-pVXZ series, the mean absolute deviations being 15.9 ($a1$), 5.5 ($a2$), 2.2 ($a3$), and 1.2 mau ($a4$) in the notation of Figs. 1 and 2. With the largest ANO set, we are not as close to the basis set limit as with the aug-cc-pV5Z set. Nevertheless, as for the DPMs, the ANO sets represent a computationally cheaper alternative to the aug-cc-pVXZ series for accurate Hartree–Fock QPMs.

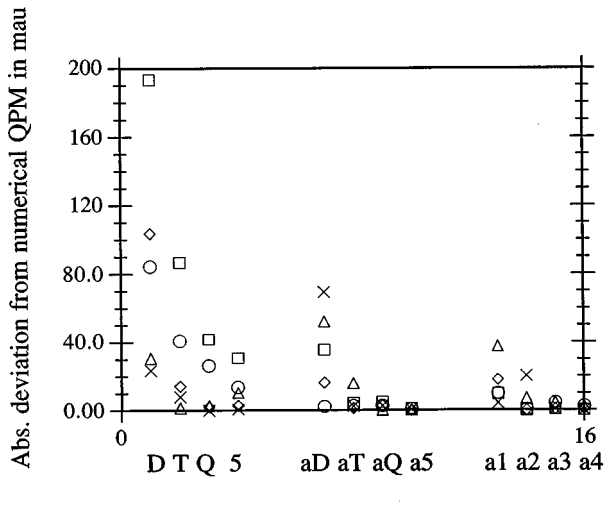

FIG. 2. The absolute value of the deviation from the numerical Hartree–Fock quadrupole moments (Ref. 24) in mau. The same abbreviations for basis sets as in Fig. 1 are used.

The differences between the cc-pVXZ and cc-pCVXZ are small for the QPM, and the same applies to the augmented versions of these series. As for the DPMs, there appears to be no urgent need for core–valence basis sets in QPM calculations on molecules containing only for first-row atoms.

The Sadlej set has a maximum error of 49.9 mau and an average error of 25.9 mau, and the accuracy is thus between that of aug-cc-pVDZ and aug-cc-pVTZ. The largest and most accurate of the Ahlrichs basis sets—TZ2P—has a maximum error of 50.2 mau and an average error of 21.9 mau. Like the Sadlej sets, the three Ahlrichs sets are thus inferior to the ANO and aug-cc-pVXZ basis sets with regards to accurate QPM calculations. The same is true for the Pople basis sets, where the largest set has maximum and mean errors of 50.2 and 23.7 mau, respectively.

From the preceding discussion, the accurate calculation of QPMs appears to be a more difficult task than the accurate calculation of DPMs. Diffuse functions are more important for describing the r_i^2 dependence of QPMs than the r_i dependence of DPMs. The discrepancies that persist between the basis set and numerical results are therefore expected to arise from an incomplete basis set description of the outer valence region. To test this conjecture, we have carried out additional calculations with the daug-cc-pVTZ and daug-cc-pVQZ basis sets, where two sets of diffuse functions have been added to the original cc-pV(T,Q)Z sets.[28] The results are given at the bottom of Table III. Significant improvements are observed when these additional diffuse functions are introduced: Going from aug-cc-pVTZ to daug-cc-pVTZ, the maximum and mean errors drop from 16.0 to 6.1 mau and

from 5.4 to 3.2 mau, respectively. For the larger quadruple-zeta sets, these errors drop from 4.8 to 2.9 mau and from 2.7 to 1.1 mau. The need for additional diffuse functions is thus clearly demonstrated.

For the DPMs, the effect of adding the same additional diffuse functions is much smaller—less than 1.5 mau at the triple-zeta level and less than 0.3 mau at the quadruple-zeta level. At the triple-zeta level, the maximum and mean error change from 1.4 to 0.8 mau and 0.9 to 0.4 mau, respectively. At the quadruple-zeta level, extremely small changes are found when adding the extra diffuse functions, which is not surprising, since we at this point have already converged to the basis set limit for all practical purposes.

3. Electric field gradient results

The Hartree–Fock EFGs are listed in Table IV(a), along with the numerical results.[24] The performance of the basis sets is rather different from that of the DPM and QPM calculations. Neither of the two valence Dunning series perform outstandingly: The average absolute errors are 26.2 and 25.5 mau, respectively, for cc-pV5Z and aug-cc-pV5Z. For each basis set, only two out of nine EFGs are within 10 mau of the numerical result and the accuracy of the EFGs is quite uneven. For the ANO sets, the situation is much the same: Only 6 calculated EFGs out of 36 are within 10 mau of the numerical results. The largest ANO set has an average absolute error of 29.2 mau and is only once within the mentioned 10 mau limit.

Clearly, with these large standard sets that performed so well for DPM and QPM, we are still far from the EFG basis set limit. Obviously, for the smaller basis sets the situation is not better. The Sadlej set performs particularly poorly (with an average absolute error of 173.2 mau) as expected for a basis set designed for flexibility in the outer valence regions rather than in the core and inner valence regions. The Pople and Ahlrichs sets are also not well suited for the calculation of EFGs, although we note that some of these sets perform as well as the considerably larger cc-pV5Z basis: For the largest Pople set, the absolute average error is 29.5 mau; for the TZ2P Ahlrichs sets, three out of nine absolute errors are below 10 mau and the average absolute error is 25.8 mau.

In Fig. 3, we have plotted the magnitude of the deviations from the numerical EFG results for the cc-pVXZ series and the core–valence series cc-pCVXZ and aug-cc-pCVXZ. These plots indicate that the two core–valence series are appropriate for EFG calculations, and that the large core–valence basis sets are the only ones that consistently yield EFGs close to the numerical values. The convergence in the cc-pCVXZ series from double-zeta to quintuple-zeta is illustrated by the following average and maximum absolute errors: 124.5 and 208.3 mau (cD), 25.4 and 43.2 mau (cT), 4.5 and 10.0 mau (cQ), and 2.7 and 4.7 mau (c5). For the aug-cc-pCVXZ series, the EFG convergence is characterized by the following average and maximum absolute errors: 102.2 and 204.8 mau (acD), 27.9 and 45.2 mau (acT), 7.1 and 19.6 mau (acQ), and 3.2 and 5.4 mau (ac5). Thus the added diffuse functions in the aug-cc-pCVXZ sets do not have a dramatic effect on the EFGs—this is not surprising since the diffuse functions are not located in the region most important for the EFG.

Although convergence is observed in Fig. 3, it is not nearly as good as for DPMs and QPMs and, for a given basis, larger fluctuations are encountered, compare Figs. 1–3. Also, the differences between the cc-pCVQZ and cc-pCV5Z sets are similar to the differences between cc-pCV5Z set and the EFG basis set limit. Since the changes from one set to the next decrease steadily throughout the cc-pCVXZ series, our results imply that, even at the next (as yet unavailable) cc-pCV6Z level, we would still not be fully converged. Noting that we already have *145 basis functions per atom* in the cc-pCV5Z basis set, it should be quite clear that EFGs are indeed particularly demanding with respect to the quality of the basis set.

To explore the requirements for high accuracy in the EFGs further, we have for this property carried out calculations with additional basis sets. Since the Ahlrichs TZ2P basis performed so well for its moderate size, we tried some larger basis sets by Ahlrichs and co-workers. The QZ2P basis set,[35] in particular, has been employed by Gauss and Stanton for accurate nuclear magnetic shielding constants[41] at the CCSD and CCSD(T) (i.e., CCSD with perturbative triples corrections[42]) levels. We have carried out EFG calculations with this basis set—alone and augmented with one set of f functions on the first-row atoms and one set of d functions on hydrogen (with exponents taken from the cc-pVTZ basis set). The results are listed in Table IV(b) together with TZ2P results for reference. For the QZ2P basis, the average absolute deviation from the numerical results is 48.2 mau and only two out of nine times does this basis improve upon TZ2P. Similarly, the QZ2P1F set only improves four TZ2P results and the average absolute deviation from the numerical results is 31.9 mau. Clearly, these two sets do not in general represent an improvement upon TZ2P.

Basis set uncontraction is a common technique for improving the description of the inner regions of a molecule. We tried this approach for the aug-cc-pCVTZ basis set. The EFGs obtained in this way are given in Table IV(b) along with the aug-cc-pCVTZ results for reference. Six out of nine times the totally uncontracted set yields results that are better than the aug-cc-pCVTZ results, but the differences are small—typically around 3 mau.

Acknowledging the success of the core–valence sets (see Fig. 3), we tried to add more tight functions to the cc-pCVTZ and cc-pCVQZ sets. For cc-pCVTZ, we added one set of s, p, and d functions to the first-row atoms and one set of s and p functions to hydrogen. The exponents of the added tight functions on hydrogen were chosen to three times the largest exponent of the given type of function. For the first row atoms the exponents were chosen to three times the largest exponents of the already included tight functions of the given type of function. For the cc-pCVQZ set, we added one set of s, p, d, and f functions to the first-row atoms and one set of s, p, and d functions to hydrogen with exponents chosen in the same way as for cc-pCVTZ. The

TABLE IV. (a) Calculated Hartree–Fock 33-component of electric field gradient tensors at the nuclei in atomic units. Numerical Hartree–Fock results from Ref. 24. (b) Difference between special basis set calculated and numerically (Ref. 24) calculated Hartree–Fock 33-component of electric field gradient tensors in atomic units.

	BF		CO		HF		NO+		N_2
(a) Basis set	B	F	C	O	H	F	N	O	N
6-311 G	−0.5002	0.8804	−1.0713	−0.5140	0.6067	3.3720	−1.6002	−0.7345	−0.2108
6-311 G**	−0.5086	0.6505	1.1192	−0.6768	0.5619	3.0709	−1.7264	−0.9608	−1.3105
6-311 G ($2d$,$2p$)	−0.5276	0.6545	−1.1362	−0.6898	0.5466	2.8614	−1.7537	−0.9921	−1.3270
6-311++G**	−0.5057	0.6841	−1.1153	−0.6480	0.5570	2.9038	−1.7245	−0.9469	−1.2893
6-311++($2d$,$2p$)	−0.5276	0.6545	−1.1362	−0.6898	0.5465	2.8616	−1.7537	−0.9921	−1.3270
DZP (Ahlrichs)	−0.4565	0.5929	−1.0032	−0.5306	0.5806	2.9563	−1.5474	−0.7879	−1.1872
TZP (Ahlrichs)	−0.5135	0.6371	−1.1233	−0.6933	0.5691	2.9300	−1.7474	−0.9889	−1.3303
TZ2P (Ahlrichs)	−0.5176	0.6269	−1.1376	−0.6985	0.5657	2.8826	−1.7777	−1.0118	−1.3574
Sadlej			−1.0449	−0.4533	0.5857	2.8771	−1.5137	−0.6570	−1.0871
ANO 4321_321	−0.5087	0.5795	−1.1161	−0.6688	0.5368	2.8602	−1.7525	−1.0134	−1.3107
ANO 5432_432	−0.5259	0.6624	−1.1514	−0.6738	0.5236	2.8865	−1.7950	−0.9981	−1.3452
ANO 6543_543	−0.5375	0.5995	−1.1667	−0.7171	0.5236	2.8616	−1.8077	−1.0441	−1.3655
ANO 7643_643	−0.5395	0.6094	−1.1705	−0.7200	0.5234	2.8634	−1.8200	−1.0501	−1.3739
cc-pVDZ	−0.4413	0.5477	−0.9877	−0.5263	0.5754	2.9563	−1.5280	−0.7647	−1.1495
cc-pVTZ	−0.5328	0.5745	−1.1396	−0.7334	0.5448	2.8728	−1.7801	−1.0442	−1.3576
cc-pVQZ	−0.5400	0.5994	−1.1735	−0.7249	0.5183	2.8613	−1.8153	−1.0479	−1.3721
cc-pV5Z	−0.5408	0.5977	−1.1715	−0.7259	0.5153	2.8491	−1.8172	−1.0532	−1.3726
aug-cc-pVDZ	−0.4489	0.5814	−1.0360	−0.5201	0.5638	2.7632	−1.5557	−0.7742	−1.1193
aug-cc-pVTZ	−0.5262	0.5891	−1.1361	−0.7208	0.5435	2.7887	−1.7784	−1.0408	−1.3518
aug-cc-pVQZ	−0.5394	0.6010	−1.1718	−0.7235	0.5183	2.8394	−1.8175	−1.0515	−1.3696
aug-cc-pV5Z	−0.5410	0.5984	−1.1714	−0.7246	0.5154	2.8459	−1.8178	−1.0523	−1.3705
cc-pCVDZ	−0.4547	0.5565	−1.0246	−0.5737	0.5759	2.9729	−1.5794	−0.8243	−1.2014
cc-pCVTZ	−0.4998	0.5714	−1.0940	−0.7057	0.5447	2.8297	−1.7319	−1.0145	−1.3146
cc-pCVQZ	−0.5165	0.5808	−1.1288	−0.7101	0.5187	2.8006	−1.7651	−1.0282	−1.3351
cc-pCV5Z	−0.5165	0.5875	−1.1311	−0.7082	0.5152	2.7965	−1.7704	−1.0293	−1.3355
aug-cc-pCVDZ	−0.4603	0.5989	−1.0595	−0.5571	0.5676	2.7778	−1.5985	−0.8278	−1.1707
aug-cc-pCVTZ	−0.4974	0.5855	−1.0904	−0.6950	0.5434	2.7654	−1.7299	−1.0082	−1.3042
aug-cc-pCVQZ	−0.5165	0.5841	−1.1284	−0.7076	0.5184	2.7792	−1.7653	−1.0274	−1.3302
aug-cc-pCV5Z	−0.5163	0.5882	−1.1310	−0.7080	0.5153	2.7934	−1.7707	−1.0295	−1.3333
Numerical h.f.	−0.5186	0.5892	−1.1343	−0.7105	0.5119	2.7988	−1.7751	−1.0326	−1.3366
(b) Basis set									
TZ2P	0.0010	0.0377	−0.0033	0.0120	0.0538	0.0838	−0.0026	0.0208	−0.0208
QZ2P	−0.0207	0.0898	−0.0285	0.0389	0.0472	0.1409	−0.0058	0.0502	−0.0118
QZ2P1F	−0.0212	0.0286	−0.0390	−0.0080	0.0216	0.0887	−0.0382	−0.0039	−0.0375
aug-cc-pCVTZ	0.0212	−0.0037	0.0439	0.0155	0.0315	−0.0334	0.0452	0.0244	0.0324
Uncontracted	0.0191	−0.0009	0.0400	0.0163	0.0316	−0.0233	0.0417	0.0244	0.0310
cc-pCVTZ	0.0188	−0.0178	0.0403	0.0048	0.0328	0.0309	0.0432	0.0181	0.0220
cc-pCVTZ+ti	−0.0052	−0.0071	0.0013	−0.0033	0.0289	0.0734	0.0086	0.0078	−0.0050
cc-pCVQZ	0.0021	−0.0084	0.0055	0.0004	0.0068	0.0018	0.0100	0.0044	0.0015
cc-pCVQZ+ti	0.0037	−0.0016	0.0027	−0.0021	0.0032	0.0199	0.0028	0.0009	−0.0031
aug-cc-pCVTZ+ti	---	---	---	---	0.0272	0.0066	---	---	---
aug-cc-pCVQZ+ti	---	---	---	---	0.0026	−0.0019	---	---	---

results obtained with these basis sets are given in Table IV(b) with the cc-pCVTZ and cc-pCVQZ results for reference.

At the triple-zeta level, the maximum and mean errors change from 43.2 to 73.4 mau and from 25.4 to 15.6 mau, respectively, when tight functions are added. At the quadruple-zeta level, the corresponding changes are from 10.0 to 19.9 mau and from 4.5 to 4.4 mau. At first glance, these results are discouraging but we note that only flourine in HF constitutes a problem. Excluding the HF results, the cc-pCVTZ+ti errors are 8.6 and 5.5 mau, respectively, whereas the cc-pCVQZ+ti errors are only 3.7 and 2.4 mau. Thus, except for HF, the results obtained with the modified triple-zeta set are of an accuracy comparable to the cc-pCVQZ results. Likewise, the results obtained with the modified quadruple-zeta set are comparable to the cc-pCV5Z results.

The difficulties encountered for the EFG at the fluorine nucleus in HF arise from the fact that the electrons in this molecule to a high degree are localized around the fluorine atom, giving the system a strong ionic character. Such an electronic structure cannot be described with the cc-pCV(T,Q)Z sets augmented with tight functions—diffuse functions are needed for a balanced description of the bonding and nuclear regions. We therefore carried out calculations on HF with the aug-cc-pCV(T,Q)Z sets augmented with tight functions chosen as described above. As shown in Table IV(b), these basis sets represent a significant improvement upon the aug-cc-pCV(T,Q)Z sets for the EFG at the fluorine atom in HF.

In conclusion, the addition of tight functions to the correlation-consistent core–valence basis sets appears to be a good way to obtain EFGs closer to the basis set limit and are

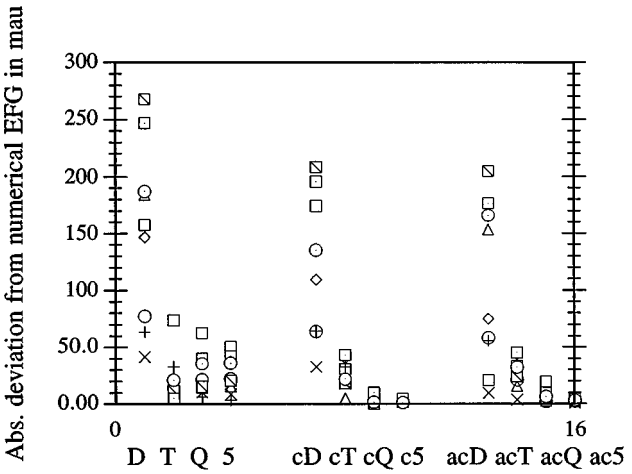

FIG. 3. The absolute value of the deviation from the numerical Hartree–Fock electric field gradients (Ref. 24) in mau. As before D is short for cc-pVDZ, and cD and acD denotes the cc-pCVDZ and aug-cc-pCVDZ basis sets, respectively.

mandatory for calculations within one thousandths of an atomic unit of the basis set limit, although a more systematic approach for selecting the exponents of the extra tight functions (as well as the number of extra tight functions) would definitely be desirable.

C. CCSD results

The calculated CCSD first-order one-electron properties are listed in Table V (DPM), Table VI (QPM), and Table VII (EFG). Comparing the uncorrelated and correlated DPMs at the aug-cc-pV5Z level in Tables II and V, we observe large variations in the correlation effects. The changes from Hartree–Fock to CCSD range from 16 to 128 mau (i.e., 4.6% to 122%). The DPM in CO, in particular, displays large correlation effects, changing the sign as we go from an uncorrelated to a correlated description. Compared with the changes in the DPMs in the aug-cc-pVXZ series at the CCSD level (Table V), we note that correlation effects are usually more important than basis set effects. Recalling that among the properties considered here, the DPM was the easiest to converge to the basis set limit at the Hartree–Fock level, this is not surprising.

A similar situation is found for the QPMs. Comparing the aug-cc-pV5Z QPMs in Tables III and VI, we find that the changes from Hartree–Fock to CCSD vary from 17 to 536 mau (i.e., from 1.0% to 18.1%). We thus have correlation effects up to 20%. Comparing with the CCSD QPM changes in the aug-cc-pVXZ series (Table VI), we note that correlation effects are more important than basis set effects for the QPMs as well.

For the EFGs, the situation is slightly different. Comparing EFGs calculated with the cc-pCV5Z basis set in Tables IV(a) and VII, we see that the changes from Hartree–Fock to CCSD vary from 12 to 312 mau (i.e., 1.8% to 18.9%). The correlation effects are typically around 10%. Compared to the CCSD EFG changes in the cc-pCVXZ series (Table VII), correlation effects are important, but basis set effects are often equally important. Consequently, basis set effects are relatively more important for EFGs than for DPMs and QPMs—as expected from the problems with basis set convergence already discussed at the Hartree–Fock level.

TABLE V. Calculated CCSD molecular electric dipole moments in atomic units.

Basis set	BF	CO	HF	NO^+
6-311G	0.1619	0.0047	−0.8739	0.1671
6-311G**	0.3519	−0.0503	−0.7477	0.1553
6-311G(2*d*,2*p*)	0.3196	−0.0350	−0.7370	0.1387
6-311++G**	0.3147	−0.0351	−0.7707	0.1453
6-311++G(2*d*,2*p*)	0.3196	−0.0350	−0.7366	0.1387
DZP (Ahlrichs)	0.3768	−0.0332	−0.7265	0.1703
TZP (Ahlrichs)	0.3150	−0.0218	−0.7686	0.1416
TZ2P (Ahlrichs)	0.3279	−0.0349	−0.7300	0.1375
Sadlej		−0.0402	−0.7068	0.1297
ANO 4321_321	0.3292	−0.0332	−0.7159	0.1403
ANO 5432_432	0.3286	−0.0294	−0.7125	0.1432
ANO 6543_543	0.3256	−0.0280	−0.7126	0.1413
ANO 7643_643	0.3258	−0.0278	−0.7128	0.1413
cc-pVDZ	0.3760	−0.0680	−0.7203	0.1570
cc-pVTZ	0.3453	−0.0428	−0.7183	0.1433
cc-pVQZ	0.3274	−0.0270	−0.7199	0.1440
cc-pV5Z	0.3241	−0.0237	−0.7213	0.1436
aug-cc-pVDZ	0.3407	−0.0383	−0.7096	0.1333
aug-cc-pVTZ	0.3272	−0.0284	−0.7124	0.1396
aug-cc-pVQZ	0.3236	−0.0244	−0.7154	0.1427
aug-cc-pV5Z	0.3232	−0.0233	−0.7165	0.1436
cc-pCVDZ	0.3751	−0.0685	−0.7209	0.1578
cc-pCVTZ	0.3388	−0.0358	−0.7189	0.1464
cc-pCVQZ	0.3263	−0.0260	−0.7200	0.1445
cc-pCV5Z	0.3229	−0.0232	−0.7212	0.1439
aug-cc-pCVDZ	0.3387	−0.0282	−0.7371	0.1345
aug-cc-pCVTZ	0.3233	−0.0266	−0.7200	0.1408
aug-cc-pCVQZ	0.3223	−0.0236	−0.7173	0.1432
aug-cc-pCV5Z	0.3222	−0.0227	−0.7172	0.1439
daug-cc-pVTZ	0.3273	−0.0293	−0.7113	0.1397
daug-cc-pVQZ	0.3238	−0.0246	−0.7153	0.1429

1. Dipole moment results

It is a little harder to converge the DPM to the basis set limit at the CCSD level than at the Hartree–Fock level. This point is illustrated in the upper third of Table VIII, where we give the absolute value of the maximum and average changes in the DPMs when going from aug-cc-pVDZ to aug-cc-pVTZ, from aug-cc-pVTZ to aug-cc-pVQZ, and from aug-cc-pVQZ to aug-cc-pV5Z. The CCSD convergence of the aug-cc-pVXZ series in Table VIII combined with the corresponding Hartree–Fock convergence (in particular the fact that we have fully converged Hartree–Fock results), suggests that, for DPMs, we are within 0.5 mau of the CCSD basis set limit results with the aug-cc-pV5Z basis set—that is, close to fully converged. In Fig. 4, the absolute value of the deviation from the aug-cc-pV5Z results is given for the same basis sets as in Fig. 1. A comparison of the Dunning series in Fig. 4 demonstrates the need for diffuse functions, without which the results become scattered and unreliable. The very good hierarchical convergence of aug-cc-pVXZ series observed at

TABLE VI. Calculated CCSD 33-component of traceless molecular electric quadrupole moment tensor in atomic units.

Basis set	BF	CO	HF	NO^+	N_2
6-311G	−2.9597	−2.0799	1.5820	0.2780	−1.9192
6-311G**	−2.6686	−1.5896	1.5841	0.2802	−1.3683
6-311G(2*d*,2*p*)	−2.6056	−1.4780	1.7014	0.4724	−1.1405
6-311++G**	−2.6139	−1.6225	1.6677	0.2810	−1.3389
6-311++G(2*d*,2*p*)	−2.6056	−1.4780	1.7019	0.4724	−1.1405
DZP (Ahlrichs)	−2.7298	−1.6313	1.5918	0.2732	−1.4179
TZP (Ahlrichs)	−2.7505	−1.6972	1.6630	0.2456	−1.4373
TZ2P (Ahlrichs)	−2.6286	−1.5063	1.6680	0.4416	−1.2125
Sadlej		−1.4592	1.7204	0.4803	−1.1368
ANO 4321_321	−2.6171	−1.5184	1.7258	0.4598	−1.1362
ANO 5432_432	−2.6367	−1.4701	1.7099	0.4521	−1.1141
ANO 6543_543	−2.6137	−1.4674	1.7042	0.4515	−1.1171
ANO 7643_643	−2.6148	−1.4658	1.7063	0.4517	−1.1168
cc-pVDZ	−2.6254	−1.5203	1.5685	0.3230	−1.3421
cc-pVTZ	−2.6076	−1.4713	1.6336	0.4277	−1.2194
cc-pVQZ	−2.6194	−1.4702	1.6665	0.4481	−1.1651
cc-pV5Z	−2.6216	−1.4751	1.6912	0.4522	−1.1490
aug-cc-pVDZ	−2.5618	−1.5350	1.7019	0.4461	−1.1084
aug-cc-pVTZ	2.6158	−1.4796	1.7114	0.4523	−1.1124
aug-cc-pVQZ	−2.6158	−1.4623	1.7164	0.4571	−1.1084
aug-cc-pV5Z	−2.6193	−1.4608	1.7153	0.4562	−1.1091
cc-pCVDZ	−2.6207	−1.5110	1.5705	0.3273	−1.3311
cc-pCVTZ	−2.6245	−1.4717	1.6318	0.4307	−1.2075
cc-pCVQZ	−2.6160	−1.4667	1.6663	0.4495	−1.1619
cc-pCV5Z	−2.6183	−1.4719	1.6912	0.4540	−1.1461
aug-cc-pCVDZ	−2.5561	−1.4903	1.7433	0.4483	−1.1050
aug-cc-pCVTZ	−2.6135	−1.4710	1.7247	0.4588	−1.1038
aug-cc-pCVQZ	−2.6124	−1.4587	1.7205	0.4591	−1.1050
aug-cc-pCV5Z	−2.6162	−1.4584	1.7162	0.4577	−1.1067
daug-cc-pVTZ	−2.6171	−1.4697	1.7152	0.4521	−1.1180
daug-cc-pVQZ	−2.6181	−1.4623	1.7155	0.4554	−1.1107

the Hartree–Fock level remains intact at the CCSD level, with the changes in the DPMs decreasing steadily as we go through the hierarchy.

At the Hartree–Fock level, the performance of the largest ANO set was similar to that of the aug-cc-pVQZ basis set. At the CCSD level, the results are closer to the aug-cc-pVTZ results: The maximum and average absolute differences from the aug-cc-pV5Z results are 4.4 and 3.3 mau, respectively—see Table V and Fig. 4. Clearly, the ANO sets do not perform so well at the correlated level as at the Hartree–Fock level. If an accuracy better than that of aug-cc-pVTZ is needed (around 5 mau from the basis set limit), then the aug-cc-pVQZ and aug-cc-pV5Z basis sets must be used at the CCSD level. The ANO sets no longer represent a less expensive alternative for the calculation of high accuracy DPMs.

The differences between the DPMs obtained with the augmented Dunning sets and the doubly augmented Dunning sets are again small—less than 1.1 mau at the triple-zeta level and less than 0.2 mau at the quadruple-zeta level (see Table V). We are thus quite close to basis set saturation with only one set of diffuse functions. All things considered, a consistent accuracy of around 5 mau within the CCSD DPM basis set limit is attainable using the aug-cc-pVTZ basis set, but for higher accuracy we must go to the aug-cc-pVQZ basis set or even further.

As at the Hartree–Fock level, the differences between DPMs obtained with the valence and core–valence Dunning series are quite small, particularly for the larger sets, where the differences usually are less than 1/2 mau. Therefore, there is no compelling reason for using the core–valence basis sets for DPM calculations on molecules containing no higher than first-row atoms.

The smallest difference between the Sadlej basis set and aug-cc-pV5Z set is 9.7 mau. In general, the Sadlej basis performs less well at the CCSD level than at the Hartree–Fock level. The differences between the TZ2P set and aug-cc-pV5Z are between 4.6 and 13.4 mau, and highly accurate DPMs cannot be obtained using the TZ2P basis set at the correlated level. The Pople results are far from the DPMs obtained with aug-cc-pV5Z, and the Pople basis sets are not well suited for accurate CCSD DPM calculations.

2. Quadrupole moment results

In the middle third of Table VIII, we list the absolute values of the maximum and average changes in the calculated CCSD QPM going from aug-cc-pVDZ to aug-cc-pVTZ, from aug-cc-pVTZ to aug-cc-pVQZ and from aug-cc-pVQZ to aug-cc-pV5Z. The CCSD convergence towards the QPM basis set limit is similar to that at the Hartree–Fock level. Comparison with the Hartree–Fock convergence indicates that we are within 2 mau of the CCSD basis set limit. At the CCSD level, QPMs are therefore more difficult to converge than DPMs, as was also true at the Hartree–Fock level.

In Fig. 5, the absolute value of the deviation from the aug-cc-pV5Z results is given for the same basis sets as in Fig. 2. The importance of diffuse basis functions for describing the r_i^2 dependence of the QPM is clearly demonstrated by the two Dunning series in Fig. 5. Without diffuse functions, the results are much too scattered to be able to make reliable judgements about the probable accuracy of a given calculation. The hierarchical structure of the aug-cc-pVXZ series is still present at the CCSD level as we observe good improvements from one basis set to the next in the series (but less satisfactory than for the DPMs, since we are not so close to the basis set limit with the largest basis set).

As for the DPMs, the ANO sets perform less well at the CCSD level than at the Hartree–Fock level. The maximum and average absolute differences between the largest ANO set and the aug-cc-pV5Z set are 8.9 and 6.2 mau, respectively. As is evident from Fig. 5, the ANO sets are still considerably more accurate than the cc-pVXZ series. However, compared with the larger aug-cc-pVXZ basis sets, the latter sets are preferable for highly accurate CCSD QPM calculations.

The results of the daug-cc-pVTZ and daug-cc-pVQZ sets are included in Table VI. As at the Hartree–Fock level, the differences between the QPMs obtained with the singly and doubly augmented Dunning sets are larger than for the DPMs. The maximum and mean deviations from the aug-cc-

TABLE VII. Calculated CCSD 33-component of electric field gradient tensors at the nuclei in atomic units.

	BF		CO		HF		NO^+		N_2
Basis set	B	F	C	O	H	F	N	O	N
6-311G	−0.4340	0.7176	−0.8894	−0.6044	0.6288	3.2849	−1.2471	−0.7867	−1.0507
6-311G**	−0.4434	0.5193	−0.9355	−0.7095	0.5854	3.0087	−1.3691	−0.9384	−1.1260
6-311G(2*d*,2*p*)	−0.4655	0.5214	−0.9581	−0.7113	0.5733	2.7267	−1.4073	−0.9651	−1.1381
6-311++G**	−0.4391	0.5526	−0.9277	−0.6698	0.5809	2.7934	−1.3649	−0.9223	−1.0934
6-311++(2*d*,2*p*)	−0.4655	0.5214	−0.9581	−0.7113	0.5733	2.7270	−1.4073	−0.9651	−1.1381
DZP (Ahlrichs)	−0.3875	0.4551	−0.8129	−0.5597	0.6030	2.8097	−1.1836	−0.7641	−0.9913
TZP (Ahlrichs)	−0.4463	0.5025	−0.9368	−0.7077	0.5956	2.8059	−1.3802	−0.9533	−1.1326
TZ2P (Ahlrichs)	−0.4512	0.4868	−0.9542	−0.7215	0.5917	2.7416	−1.4188	−0.9800	−1.1648
Sadlej			−0.8488	−0.5259	0.6133	2.6041	−1.1526	−0.6680	−0.8898
ANO 4321_321	−0.4383	0.4384	−0.9287	−0.6757	0.5628	2.6800	−1.3867	−0.9560	−1.1011
ANO 5432_432	−0.4646	0.5245	−0.9775	−0.6968	0.5464	2.7164	−1.4551	−0.9692	−1.1590
ANO 6543_543	−0.4805	0.4728	−0.9972	−0.7339	0.5455	2.6942	−1.4709	−1.0104	−1.1794
ANO 7643_643	−0.4832	0.4832	−1.0013	−0.7370	0.5451	2.7023	−1.4828	−1.0161	−1.1883
cc-pVDZ	−0.3694	0.4128	−0.7905	−0.5566	0.5968	2.8217	−1.1605	−0.7422	−0.9530
cc-pVTZ	−0.4704	0.4514	−0.9645	−0.7488	0.5693	2.7566	−1.4359	−1.0050	−1.1723
cc-pVQZ	−0.4860	0.4775	−1.0104	−0.7410	0.5383	2.7125	−1.4860	−1.0158	−1.1935
cc-pV5Z	−0.4913	0.4802	−1.0153	−0.7400	0.5337	2.6890	−1.4951	−1.0217	−1.1976
aug-cc-pVDZ	−0.3789	0.4201	−0.8455	−0.5498	0.5896	2.5392	−1.2008	−0.7521	−0.9219
aug-cc-pVTZ	−0.4640	0.4558	−0.9610	−0.7357	0.5687	2.6236	−1.4362	−1.0040	−1.1628
aug-cc-pVQZ	−0.4858	0.4757	−1.0090	−0.7389	0.5387	2.6685	−1.4888	−1.0194	−1.1896
aug-cc-pV5Z	−0.4917	0.4787	−1.0157	−0.7388	0.5340	2.6764	−1.4965	−1.0213	−1.1951
cc-pCVDZ	−0.3848	0.4238	−0.8311	−0.6063	0.5967	2.8524	−1.2161	−0.8038	−1.0084
cc-pCVTZ	−0.4454	0.4542	−0.9340	−0.7240	0.5677	2.7232	−1.4091	−0.9829	−1.1410
cc-pCVQZ	−0.4667	0.4684	−0.9746	−0.7234	0.5379	2.6647	−1.4488	−0.9960	−1.1635
cc-pCV5Z	−0.4691	0.4764	−0.9807	−0.7206	0.5332	2.6455	−1.4584	−0.9980	−1.1657
aug-cc-pCVDZ	−0.3910	0.4383	−0.8738	−0.5895	0.5919	2.5699	−1.2476	−0.8076	−0.9761
aug-cc-pCVTZ	−0.4431	0.4578	−0.9305	−0.7126	0.5674	2.6112	−1.4089	−0.9777	−1.1274
aug-cc-pCVQZ	−0.4665	0.4676	−0.9745	−0.7210	0.5379	2.6208	−1.4498	−0.9959	−1.1570
aug-cc-pCV5Z	−0.4689	0.4752	−0.9808	−0.7106	0.5334	2.6339	−1.4589	−0.9985	−1.1626
''cc-pCVTZ+ti''	−0.4659	0.4638	−0.9659	−0.7325	0.5630	2.6515	−1.4357	−0.9929	−1.1639
''cc-pCVQZ+ti''	−0.4660	0.4746	−0.9778	−0.7262	0.5343	2.6381	−1.4554	−0.9998	−1.1677

pV5Z set change from 18.8 to 9.0 mau and 6.7 to 4.9 mau, respectively, when going from aug-cc-pVTZ to daug-cc-pVTZ. At the quadruple-zeta level, the corresponding changes are from 3.4 to 1.7 mau and from 1.5 to 1.1 mau. Again we observe a good improvement in the QPMs when more diffuse functions are added, especially in the maximum deviation. All things considered, at the daug-cc-pVTZ level, we obtain a consistent accuracy of around 10 mau within the CCSD QPM basis set limit and for higher accuracy we must go at least to the aug-cc-pVQZ basis.

TABLE VIII. Absolute value in mau of the maximum and mean changes in: upper third) DP when going from aug-cc-pVDZ to aug-cc-pVTZ, from aug-cc-pVTZ to aug-cc-pVQZ, and from aug-cc-pVQZ to aug-cc-pV5Z, middle third) QP when going from aug-cc-pVDZ to aug-cc-pVTZ, from aug-cc-pVTZ to aug-cc-pVQZ, and from aug-cc-pVQZ to aug-cc-pV5Z, lower third) EFG when going from cc-pCVDZ to cc-pCVTZ, from cc-pCVTZ to cc-pCVQZ, and from cc-pCVQZ to the cc-pCV5Z.

	Hartree–Fock		CCSD	
	Maximum	Mean	Maximum	Mean
ABS(DP(T)-DP(D))	10.5	4.7	13.5	8.1
ABS(DP(Q)-DP(T))	1.2	0.8	4.0	3.5
ABS(DP(5)-DP(Q))	0.2	0.1	1.1	0.9
ABS(QP(T)-QP(D))	67.0	30.0	55.4	25.8
ABS(QP(Q)-QP(T))	15.6	3.6	17.3	5.2
ABS(QP(5)-QP(Q))	3.6	2.2	3.4	1.5
ABS(EFG(T)-EFG(D))	190.2	99.1	193.0	108.3
ABS(EFG(Q)-EFG(T))	34.8	20.9	58.6	26.7
ABS(EFG(5)-EFG(Q))	6.7	2.4	19.2	6.3

The larger core–valence sets typically deviate by 2 to 3 mau from their valence counterparts, so core contributions to the QPM are not extremely important for molecules containing only first-row atoms.

The Sadlej basis set gives QPMs that differ between 1.6 and 27.7 mau from the aug-cc-pV5Z basis set. The accuracy of the Sadlej set is fluctuating and too low to yield consistently accurate QPMs. The same is true for the Ahlrichs sets—the TZ2P QPMs differ between 9.3 and 103.4 mau from aug-cc-pV5Z. Finally, the Pople basis set results are far from the aug-cc-pV5Z results and cannot be used for accurate CCSD QPM calculations.

3. Electric field gradient results

As noted in the section on Hartree–Fock calculations, the only standard basis sets yielding consistently accurate EFGs at the Hartree–Fock level are the larger sets in the two Dunning core–valence series. We therefore concentrate on these two series here. In the lower third of Table VIII, we give the absolute value of the maximum and average changes in the calculated EFGs when going from cc-pCVDZ to cc-

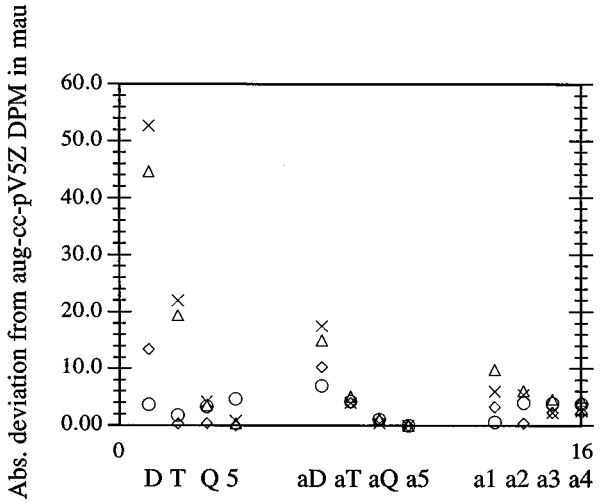

FIG. 4. The absolute value of the deviation from the calculated aug-cc-pV5Z CCSD dipole moments in mau. The same abbreviations for basis sets as in Fig. 1 are used.

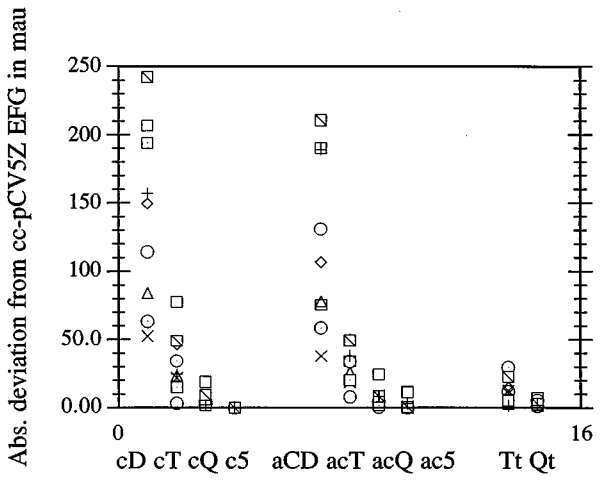

FIG. 6. The absolute value of the deviation from the calculated cc-pCV5Z CCSD electric field gradients in mau. The same abbreviations for the core-valence basis sets as in Fig. 3 are used. Tt and Qt are short for the cc-pCVTZ+ti and cc-pCVQZ+ti basis sets, respectively.

pCVTZ, from cc-pCVTZ to cc-pCVQZ, and from cc-pCVQZ to cc-pCV5Z. As is readily seen, the EFGs are harder to converge towards the basis set limit at the CCSD level than at the Hartree–Fock level. This circumstance emphasizes the problems already observed with basis set convergence of the EFGs at the Hartree–Fock level, where the most accurate basis set (cc-pCV5Z) was almost 3 mau from the basis set limit.

The EFG results are displayed in Fig. 6, where the absolute value of the deviation from the cc-pCV5Z results are given for the two core–valence series. As in the Hartree–Fock calculations, the differences between the cc-pCVXZ and aug-cc-pCVXZ results are not large (typically less than 2 mau for the larger sets in the series, although larger differences do appear). Although both core–valence series show some hierarchical characteristics, they are not as good as the aug-cc-pVXZ series for the DPM and QPM calculations, with considerable scattering persisting even at the quadruple-zeta level. Thus although we note some converging trends in Fig. 6 and in Table VIII, we conclude that we are still some distance away from the CCSD EFG basis set limit with the cc-pCV5Z and aug-cc-pCV5Z basis sets. It is difficult to state precisely how far away we are, but up to 10 mau is definitely possible.

In Fig. 6, we have also included the results obtained with the specially constructed basis sets cc-pCVTZ+ti (Tt) and cc-pCVQZ+ti (Qt), where tight functions have been added to the cc-pCVTZ and cc-pCVQZ sets. For the HF molecule, the results given in Table VII and Fig. 6 are obtained with the modified aug-cc-pCVTZ and aug-cc-pCVQZ sets, consistent with the discussion above. The inclusion of tight functions improves the results but less so than at the Hartree–Fock level, again illustrating the fact that EFGs are harder to compute accurately at the CCSD level than at the Hartree–Fock level.

The EFGs are clearly a very challenging property. With the most accurate basis sets, we are only able to obtain results consistently within 5 mau of the basis set limit at the Hartree–Fock level. Even this accuracy is not possible to achieve at the CCSD level, where the most accurate results are as much as 10 mau away from the basis set limit. Although we have seen that the core–valence sets take us in the right direction, we have also found that they do not take us all the way to the basis set limit. To eliminate the remaining error, we must design better basis sets with a more flexible description of the core and inner valence regions. Our results with the cc-pCVTZ+ti and cc-pCVQZ+ti basis sets indicate that one possibility would be to extend the cc-pCVXZ basis sets by adding more tight functions. Such basis sets will

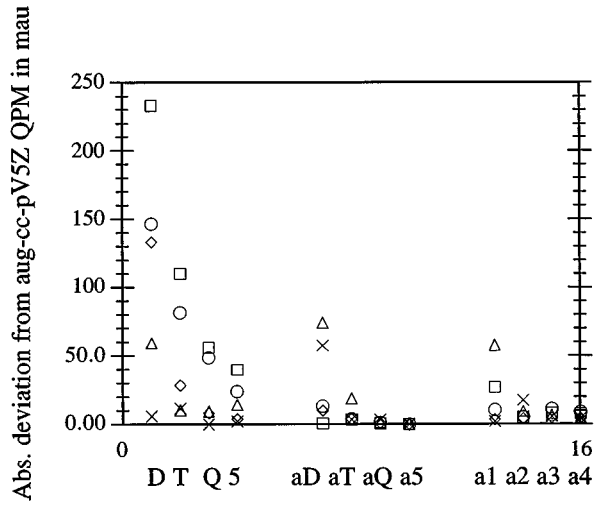

FIG. 5. The absolute value of the deviation from the calculated aug-cc-pV5Z CCSD quadrupole moments in mau. The same abbreviations for basis sets as in Fig. 1 are used.

TABLE IX. Calculated 33-component of the electric field gradient tensors at the nuclei in hydrogen cyanid at the Hartree–Fock and CCSD level in atomic units.

	H		C		N	
Basis set	Hartree–Fock	CCSD	Hartree–Fock	CCSD	Hartree–Fock	CCSD
pCVTZ	0.3229	0.3253	−0.4413	−0.3433	−1.1487	−0.9839
pCVQZ	0.3174	0.3173	−0.4699	−0.3761	−1.1649	−1.0024
pCV5Z	0.3164	0.3156	−0.4715	−0.3809	−1.1665	−1.0054
aug-pCVTZ	0.3236	0.3259	−0.4429	−0.3471	−1.1427	−0.9762
aug-pCVQZ	0.3174	0.3173	−0.4710	−0.3782	−1.1638	−1.0008
aug-pCV5Z	0.3163	0.3156	−0.4716	−0.3815	−1.1665	−1.0055
pCVTZ+ti	0.3220	0.3243	−0.4699	−0.3669	−1.1727	−1.0043
pCVQZ+ti	0.3155	0.3157	−0.4708	−0.3775	−1.1698	−1.0069

become very large, implying that high-accuracy EFG calculations will be reserved fairly small systems.

IV. ELECTRIC FIELD GRADIENTS IN HYDROGEN CYANIDE

Several theoretical studies of the EFGs in HCN have been carried out.[43–46] We have used the same geometry as Cremer *et al.* and Bishop *et al.*: $R(\mathrm{CN}) = 1.1532$ Å and $R(\mathrm{HC}) = 1.0655$ Å.[45,46] Cummins *et al.* used a slightly shorter bond length $R(\mathrm{CN}) = 1.1484$ Å for the CN bond, whereas Scuseria *et al.* have used $R(\mathrm{CN}) = 1.163$ Å and $R(\mathrm{HC}) = 1.068$ Å.[44,43]

We have used the three largest core–valence and augmented core–valence basis sets as well as the modified core–valence sets cc-pCVTZ+ti and cc-pCVQZ+ti discussed above. The Hartree–Fock and CCSD results are given in Table IX. Our primary interest is the comparison with the other theoretical investigations, which have focused entirely on the EFG at the nitrogen nucleus. We therefore restrict our attention to the nitrogen atom.

Comparing the Hartree–Fock EFG changes in the two core–valence series with the changes in Table VIII, we note that the convergence for the EFG at the nitrogen atom in HCN is better than average. Taking into account the monotonical convergence in Table IX and the fact that our previous investigations showed cc-pCV5Z to be consistently within 5 mau of the Hartree–Fock limit, we estimate the Hartree–Fock limit of the nitrogen EFG to be -1.169 ± 0.005 a.u., by retaining an uncertainty of 5 mau and subtracting half of this uncertainty from the cc-pCV5Z result. Comparing the changes at the CCSD level in the two core–valence series with the ones in Table VIII, we also note that the convergence at the CCSD level is better than average. From this (comparatively) good convergence combined with the above-mentioned possible CCSD basis set limit error of up to 10 mau, we estimate the CCSD limit of the nitrogen EFG in HCN to be -1.010 ± 0.010 a.u. in the same way as at the SCF level.

In Table X, we give our Hartree–Fock and CCSD results together with the results of the other investigations: The Hartree–Fock and configuration-interaction singles and doubles (CISD) results of Scuseria *et al.*,[43] the Hartree–Fock and coupled pair-functional (CPF) results of Cummins *et al.*,[44] the Hartree–Fock and MP2 results of Bishop *et al.*,[46] and the Hartree–Fock, Møller–Plesset (MP2, MP3, MP4), quadratic configuration-interaction singles and doubles (QCISD), and QCISD augmented by perturbative corrections for triple excitations (QCISD(T)) results of Cremer *et al.*[45]

The differences between the CCSD, CISD, CPF, and QCISD results are not large, but we regard our CCSD results as the most reliable since we have carried out several calculations in large, accurate basis sets, enabling us to make a

TABLE X. Comparison of the calculated 33-component of the electric field gradient tensor at the nitrogen nuclei in HCN with various other theoretical studies. All results are in atomic units.

		EFG(N)		
Method	Basis set	Hartree–Fock	Correlated	Reference
Hartree–Fock/CCSD[a]	Estimated basis set limit	−1.169(5)	−1.01(1)	Present work
Hartree–Fock/CISD	Huzinaga/Dunning TZ+2P	−1.140	−1.000	43
Hartree–Fock/CPF	Huzinaga, [6 4 2 1/4 2 1]	−1.1961	−0.998	44
Hartree–Fock/MP2[b]	[12 8 4 2/8 5 1]	−1.201	−0.9463	46
Hartree–Fock/MP2,	6-311G(2*d*,2*p*)	−1.173	−0.942	45
MP3,			−1.033	
MP4,			−0.955	
QCISD,			−1.001	
QCISD(T)			−0.977	

[a]Estimated basis set limit results with uncertainty on the last digit in parentheses.
[b]Extended Van Duijneveldt basis set.

TABLE XI. Theoretically calculated and experimentally measured DPM of furan in Debye.

Method	Basis set	DPM		Reference
		Hartree–Fock	Correlated	
Hartree–Fock/CCSD	aug-cc-pVDZ	0.805	0.683	Present work
Hartree–Fock/CCSD	aug-cc-pVTZ	0.790	0.704	Present work
MRCI	Huzinaga/Dunning DZP		0.716	50
MRCI	Dunning TZVP		0.752	50
MP2	6-31G*		0.755	48
CASPT2[a]	C,O[4*s*3*p*1*d*]/H[2*s*1*p*]		0.928	49
CASPT2[b]	C,O[4*s*3*p*1*d*]/H[2*s*1*p*]		0.971	49
Experiment[c]	-----		0.661(6)	51

[a](0064) active space.
[b](4232) active space.
[c]Microwave spectroscopy study, the uncertainty on the last digit is given in parenthesis.

reliable estimate of the basis set limit. Cummins *et al.* and Cremer *et al.* correct their correlated results for basis set incompleteness errors, estimating the basis set error at the Hartree–Fock level and adding this correction to the correlated results. This approach is not rigorous and can only give an order-of-magnitude estimate of the error, as our investigations clearly have demonstrated that the EFG basis set errors are different at the uncorrelated and correlated levels. In addition, there is the difficulty in establishing the Hartree–Fock limit. Sundholm *et al.* have calculated the basis set limit for the CN^- system[24] and Cummins *et al.* have carried out calculations on CN^- as well. Having established the Hartree–Fock correction for CN^-, they carry on to use this value for HCN as well, because of the obvious similarities between the two systems. Although in general the validity of this approach is questionable, it works in this case since the corrected Hartree–Fock result for HCN is -1.168 mau, in excellent agreement with our estimated basis set limit. Cremer *et al.* use as the Hartree–Fock limit the results of Cummins *et al.* in Table X. However, Cummins *et al.* correct their result quite a bit (28 mau), and the correction of 23 mau that Cremer *et al.* apply cannot be trusted as a reliable correction for the basis set error.

Although our integral-direct implementation has given us the ability to estimate the CCSD EFG basis set limit reliably, there is still room for improvement. The effects of higher-order excitations in the cluster operator are not negligible as is seen from the QCISD and QCISD(T) results in Table X, where the perturbative triples correction amounts to 24 mau. Although we cannot reliably correct our CCSD limit result by this amount [obtained using a *6-311*G(2*d*,2*p*) basis], it may still serve as a rough estimate of the triples corrections. To obtain highly accurate EFGs, it is thus necessary to employ large basis sets including tight functions and to consider correlation effects beyond CCSD.

Finally, from the Møller–Plesset results by Cremer *et al.* in Table X, we note that the perturbation series oscillates—a common situation in Møller–Plesset series. Second-order Møller–Plesset theory overestimates the correlation effects (most accurately described by the QCISD(T) calculation of Cremer *et al.*), third-order theory overcorrects back and so on.

V. THE DIPOLE MOMENT OF FURAN

Furan is a planar aromatic heterocyclic molecule that possesses C_{2v} symmetry. In our calculations of the dipole moment of furan we have used the experimentally determined ground-state equilibrium geometry,[47] and arranged the molecule in a coordinate system such that a positive DPM corresponds to the negative end of the dipole being located at the oxygen atom. We have calculated the DPM in both the aug-cc-pVDZ and aug-cc-pVTZ basis sets, which give rise to 151 and 322 basis functions, respectively, so considering the results of the basis set investigation above, we expect the basis set error to be small in the largest calculation. In Table XI we give our calculated DPMs along with the results of other theoretical studies[48–50] and the experimentally determined value[51] of 0.661 ± 0.006 D (1 D = 2.541 77 a.u.) from microwave spectroscopy.

We first note that the changes in the DPM with the basis set in our calculations are similar to the changes found for the diatomics above, with changes from aug-cc-pVDZ to aug-cc-pVTZ of 6 and 8 mau at the SCF and CCSD levels, respectively (remembering $1\ \mathrm{D} = 2.541\ 77$ a.u.). We therefore believe the basis set error at the CCSD/aug-cc-pVTZ to be similar to the error found for the diatomics at the same level, and we thus expect the value of 0.704 D to be, at least, within 0.02 D of the CCSD basis set limit. We also note that increasing the basis set results in an increase in the DPM. This trend is also observed for the multireference configuration interaction results of Palmer *et al.*[50]

Based solely on experimental techniques it has not been possible to determine the sign of the DPM of furan.[50,52] However, from our results there can be no doubt that the negative end of the dipole is located at the oxygen atom. A qualitatively interpretation of this is that the inductive effect originating from the difference in electronegativity between oxygen and carbon thus is larger than the effect of electron donation from the oxygen lone-pair to the conjugated pi-electron system.

From Table XI we further see that the DPM obtained using the integral-direct CCSD algorithm is closer to the experimental value than any of the other theoretical values. Furthermore our value of 0.704 D is in a sense more reliable

than the other theoretical values as the integral-direct implementation has enabled us to employ accurate basis sets, which yields results close to the basis set limit. The SCF/aug-cc-pVTZ DPM is 129 mD (19.5%) away from the experimental value but CCSD in the same basis set is able to narrow this value down to 43 mD (6.5%). The difference from theory to experiment is thus reduced by a factor of 3 when going from SCF to CCSD. However, we do not end up with a DPM within the error bars of the experimental value with the integral-direct CCSD model. However, we have not considered the effect of higher order excitations in the cluster operator (especially triple excitations) or rotational–vibrational averaging of the experimental value, and we attribute the remaining discrepancy between our CCSD value and the experimental value to these two effects.

In conclusion, our results therefore show that for ''larger'' chemical systems like furan, the integral-direct CCSD model takes us the important step from the qualitative agreement with experiment that is obtained at the SCF level to a level with semiquantitative to quantitative agreement. Furthermore, the importance of including higher order excitations in the cluster operator in an integral-direct fashion for high accuracy studies of large molecules has again been illustrated.

VI. CONCLUDING REMARKS

In this paper, we have presented an integral-direct implementation of CCSD first-order one-electron properties. The implementation has taken calculations of CCSD first-order one-electron properties beyond 400 basis functions, which opens new territory for accurate correlated calculations. More reliable conclusions on theoretical grounds can now be drawn as the most elaborate basis sets can be employed in CCSD first-order one-electron property calculations on small molecules as illustrated by the basis set investigation and the calculations of the EFGs in HCN. Furthermore it is for larger molecules possible to perform calculations that agree semiquantitative to quantitative with the experimental values as illustrated by the DPM calculations on furan.

We have used the implementation to perform a very systematic basis set investigation for the dipole moment (DPM), the quadrupole moment (QPM), and the electric field gradient (EFG) at the Hartree–Fock and CCSD levels with calculations involving up to 362 basis functions. Basis sets of polarized triple-zeta quality with additional functions added depending on the one-electron property in question are the smallest to be recommended.

At the Hartree–Fock level we have benchmarked the basis sets against numerical results, which has given us the convergence of the different series of basis sets towards the exact Hartree–Fock basis set limit. By comparing the convergence at the CCSD and Hartree–Fock level we have obtained a reliable estimate of the CCSD basis set limit and hence the convergence towards this limit.

For the DPM, the inclusion of diffuse functions is necessary to obtain small basis set errors. The aug-cc-pVXZ series represents an excellent hierarchy for DPM calculations. At the aug-cc-pV5Z level, the DPMs are fully converged to the Hartree–Fock limit to four decimal points. At the CCSD level, the aug-cc-pVTZ set gives DPMs approximately 5 mau from the basis set limit and the accuracy improves steadily as we go through the basis set hierarchy. At the aug-cc-pV5Z level, the calculated DPMs are within 1/2 mau of the CCSD limit.

For the QPM, it is even more important to include diffuse functions in the basis set. The aug-cc-pVXZ series again represents a good hierarchy for property calculations. At the Hartree–Fock level, the basis set error of the aug-cc-pV5Z set is around 1 mau. The doubly augmented daug-cc-pVXZ sets give more accurate results than their singly augmented counterparts and at the CCSD level, the daug-cc-pVTZ set has a basis set error of around 10 mau. For higher accuracy, one must employ the larger singly and doubly augmented basis sets. The aug-cc-pV5Z set, for instance, gives results that are within 2 mau of the CCSD QPM basis set limit.

For the EFG, it is essential to include tight functions in the basis set to obtain results close to the basis set limit. Among the standard basis sets, the cc-pCV5Z basis shows the smallest basis set error—within 5 and an estimated 10 mau of the Hartree–Fock and CCSD limits, respectively. Compared to the correlation-consistent valence basis sets, the core–valence sets represent a significant step in the right direction. However, even the largest core–valence sets have some way to go before basis set limit results are obtained for EFGs. Preliminary calculations using modified core–valence basis sets indicate that significant improvements are obtained with sets augmented with multiple sets of tight functions.

As another application we have calculated the DPM of furan. From experiment alone the sign of the DPM of furan cannot be determined, but our calculations have incontestably determined this to be with the negative end at the oxygen atom. Furthermore, our numerical value compares well with the experimental value, demonstrating that within the integral-direct CCSD model it is possible to obtain semiquantitative to quantitative accuracy of DPMs for ''larger'' chemical systems of the size of furan.

As a third application we have calculated the nitrogen EFG in HCN in CCSD calculations with up to 417 basis functions, further illustrating the large-scale applicability of the present implementation. The integral-direct implementation has given us the possibility to carry out a sequence of accurate calculations, which—in combination with our experience from the basis set investigation—has enabled us to reliably estimate the CCSD limit. For small systems containing up to four atoms, we believe that the present approach—relying on sequences of systematic calculations within well-defined hierarchies of basis sets—represents the best approach with respect to control of accuracy and error estimation. Although large parts of the dynamical correlation effects are recovered at the CCSD level, correlation effects beyond CCSD are not negligible for the EFG. Therefore, steps have already been taken to implement first-order one-electron properties at the CCSD(T) level in an integral-direct fashion.

ACKNOWLEDGMENTS

One of us (A.H.) would like to thank Kenneth Ruud and Peter R. Taylor for useful discussions. This work has been supported by the Danish Research Council (Grant No. 11-0924).

APPENDIX

1. Final expression in the reduction of Eqs. (18) and (19)

The single excitation part of the transformed vector is given as

$$\rho_i^a=\rho_{i,A}^a+\rho_{i,B}^a+\rho_{i,C}^a+\rho_{i,D}^a+\rho_{i,E}^a+\rho_{i,F}^a+\rho_{i,G}^a, \tag{A1}$$

where the seven terms $A-G$ are given as

$$\rho_{i,A}^a=\sum_{bk}\ \zeta_k^b\left\{\hat{L}_{bkia}+\sum_{dl}\ (2t_{kl}^{bd}-t_{lk}^{bd})\hat{L}_{ldia}\right\}, \tag{A2}$$

$$\rho_{i,B}^a=\sum_{b}\ \zeta_i^b\left(\hat{F}_{ba}-\sum_{dkl}\ t_{lk}^{db}\hat{L}_{ldka}\right)-\sum_{j}\ \zeta_j^a\left(\hat{F}_{ij}+\sum_{bdk}\ t_{jk}^{db}\hat{L}_{kbid}\right), \tag{A3}$$

$$\rho_{i,C}^a=\sum_{ef}\ \hat{L}_{feia}\sum_{dkl}\ \zeta_{kl}^{df}t_{kl}^{de}-\sum_{lj}\ \hat{L}_{ljia}\sum_{dek}\ \zeta_{kj}^{de}t_{kl}^{de}, \tag{A4}$$

$$\rho_{i,D}^a=-\sum_{e}\ \hat{F}_{ie}\sum_{dkl}\ \zeta_{kl}^{da}t_{kl}^{de}-\sum_{l}\ \hat{F}_{la}\sum_{dek}\ \zeta_{ki}^{de}t_{kl}^{de}, \tag{A5}$$

$$\rho_{i,E}^a=\sum_{dke}\ \zeta_{ki}^{de}\hat{g}_{dkea}-\sum_{dkl}\ \zeta_{kl}^{da}\hat{g}_{dkil}, \tag{A6}$$

$$\rho_{i,F}^a=\sum_{dke}\ \zeta_{ki}^{de}\left(\sum_{jf}\ t_{kj}^{df}\hat{L}_{jfea}-\sum_{jf}\ t_{jk}^{ef}\hat{g}_{jadf}-\sum_{jf}\ t_{jk}^{df}\hat{g}_{jfea}+\sum_{jl}\ t_{jl}^{de}\hat{g}_{jkla}\right), \tag{A7}$$

$$\rho_{i,G}^a=\sum_{dkl}\ \zeta_{kl}^{da}\left(-\sum_{jf}\ t_{kj}^{df}\hat{L}_{jfil}+\sum_{jf}\ t_{jl}^{df}\hat{g}_{jkif}+\sum_{jf}\ t_{jk}^{df}\hat{g}_{jfil}-\sum_{ef}\ t_{kl}^{fe}\hat{g}_{dfie}\right), \tag{A8}$$

with the L integrals and inactive Fock matrix build from modified integrals given as

$$\hat{L}_{pqrs}=2\hat{g}_{pqrs}-\hat{g}_{psrq};\hat{F}_{pq}=\hat{h}_{pq}+\sum_{k}\ \hat{L}_{kkpq}. \tag{A9}$$

The double excitation part of the transformed vector is given as

$$\rho_{ij}^{ab}=p_{ij}^{ab}(\rho_{ij,A}^{ab}+\rho_{ij,B}^{ab}+\rho_{ij,C}^{ab}+\rho_{ij,D}^{ab}+\rho_{ij,E}^{ab}+\rho_{ij,F}^{ab}+\rho_{ij,G}^{ab}+\rho_{ij,H}^{ab}), \tag{A10}$$

where the action of the permutation operator is defined by

$$P_{ij}^{ab}\begin{pmatrix}ab\\ij\end{pmatrix}=\begin{pmatrix}ab\\ij\end{pmatrix}+\begin{pmatrix}ba\\ji\end{pmatrix}, \tag{A11}$$

and the eight terms $A-H$ are given as

$$\rho_{ij,A}^{ab}=\tfrac{1}{2}\sum_{mn}\ \zeta_{mn}^{ab}\left(\hat{g}_{jnim}+\sum_{ef}\ t_{nm}^{fe}\hat{g}_{jfie}\right), \tag{A12}$$

$$\rho_{ij,B}^{ab}=\tfrac{1}{2}\sum_{cd}\ \zeta_{ij}^{cd}\hat{g}_{cadb}, \tag{A13}$$

$$\rho_{ij,C}^{ab}=-\tfrac{1}{2}\sum_{em}\ (2\zeta_{mj}^{ae}+\zeta_{jm}^{ae})\left(\hat{g}_{imeb}-\sum_{fn}\ t_{nm}^{ef}\hat{g}_{nbif}\right), \tag{A14}$$

$$\rho_{ij,D}^{ab}=\tfrac{1}{2}(2-P_{ij})\sum_{em}\ \zeta_{im}^{ae}\times\left(\hat{L}_{emjb}+\sum_{fn}\ (2t_{mn}^{ef}-t_{nm}^{ef})\hat{L}_{nfjb}\right), \tag{A15}$$

$$\rho_{ij,E}^{ab}=\tfrac{1}{2}\sum_{cd}\ \zeta_{ij}^{cd}\sum_{mn}\ t_{mn}^{cd}\hat{g}_{manb}, \tag{A16}$$

$$\rho_{ij,F}^{ab}=-\sum_{n}\ \hat{L}_{ianb}\sum_{efm}\ \zeta_{mj}^{ef}t_{mn}^{ef}-\sum_{f}\ \hat{L}_{ifjb}\sum_{emn}\ \zeta_{mn}^{ea}t_{mn}^{ef}, \tag{A17}$$

$$\rho_{ij,G}^{ab}=\sum_{e}\ \zeta_{ij}^{ae}\left(\hat{F}_{eb}-\sum_{fmn}\ t_{nm}^{fe}\hat{L}_{nfmb}\right)-\sum_{n}\ \zeta_{in}^{ab}\left(\hat{F}_{jn}+\sum_{efm}\ t_{nm}^{fe}\hat{L}_{meif}\right), \tag{A18}$$

$$\rho_{ij,H}^{ab}=2\zeta_i^a\hat{F}_{jb}-\zeta_j^a\hat{F}_{ib}+\sum_{c}\ \zeta_j^c\hat{L}_{cbia}-\sum_{k}\ \zeta_k^a\hat{L}_{jbik}, \tag{A19}$$

where P_{ij} permutes indices i and j.

2. Final expression for the right-hand side of Eq. (13)

Introducing the T_1-similarity transformed Hamiltonian we get

$$-\langle\mathrm{HF}|[H,\tau_\nu]|\mathrm{CC}\rangle=-\langle\mathrm{HF}|[\hat{H},\tau_\nu]\exp(T_2)|\mathrm{HF}\rangle=-\langle\mathrm{HF}|[\hat{H},\tau_\nu]|\mathrm{HF}\rangle \tag{A20}$$

and for the single and double excitation parts we get, respectively,

$$-\langle\mathrm{HF}|[H,\tau_1]|\mathrm{CC}\rangle=-2\hat{F}_{ia};-\langle\mathrm{HF}|[H,\tau_2]|\mathrm{CC}\rangle=-2\hat{L}_{iajb}. \tag{A21}$$

[1] G. D. Purvis and R. J. Bartlett, J. Chem. Phys. **76**, 1910 (1982).
[2] T. J. Lee and J. E. Rice, Chem. Phys. Lett. **150**, 406 (1988).
[3] G. E. Scuseria, C. L. Janssen, and H. F. Schaefer III, J. Chem. Phys. **89**, 7382 (1988).
[4] J. F. Stanton, J. Gauss, J. D. Watts, and R. J. Bartlett, J. Chem. Phys. **94**, 4334 (1991).
[5] C. Hampel, K. A. Peterson, and H.-J. Werner, Chem. Phys. Lett. **190**, 1 (1992).

[6] H. Koch, H. J. Aa. Jensen, P. Jørgensen, and T. Helgaker, J. Chem. Phys. **93**, 3345 (1990).
[7] H. Koch, R. Kobayashi, A. Sanchez de Meras, and P. Jørgensen, J. Chem. Phys. **100**, 4393 (1994).
[8] A. C. Sheiner, G. E. Scuseria, T. J. Lee, J. E. Rice, and H. F. Schaefer III, J. Chem. Phys. **87**, 5361 (1987).
[9] J. Gauss, J. F. Stanton, and R. J. Bartlett, J. Chem. Phys. **95**, 2623 (1991).
[10] H. Koch, H. J. Aa. Jensen, P. Jørgensen, T. Helgaker, G. E. Scuseria, and H. F. Schaefer III, J. Chem. Phys. **92**, 4924 (1990).
[11] H. Sekino and R. J. Bartlett, J. Chem. Phys. **98**, 3022 (1993).
[12] R. Kobayashi, H. Koch, and P. Jørgensen, Chem. Phys. Lett. **219**, 30 (1994).
[13] H. Sekino and R. J. Bartlett, Chem. Phys. Lett. **234**, 87 (1995).
[14] R. Kobayashi, R. D. Amos, H. Koch, and P. Jørgensen, Chem. Phys. Lett. **253**, 373 (1996).
[15] J. Gauss and J. F. Stanton, J. Chem. Phys. **102**, 251 (1995).
[16] J. Gauss and J. F. Stanton, J. Chem. Phys. **103**, 3561 (1995).
[17] M. Bühl, J. Gauss, and J. F. Stanton, Chem. Phys. Lett. **241**, 248 (1995).
[18] H. Koch, O. Christiansen, R. Kobayashi, P. Jørgensen, and T. Helgaker, Chem. Phys. Lett. **228**, 233 (1994).
[19] H. Koch, A. Sanchez de Meras, T. Helgaker, and O. Christiansen, J. Chem. Phys. **104**, 4157 (1996).
[20] O. Christiansen, H. Koch, A. Halkier, P. Jørgensen, T. Helgaker, and A. Sanchez de Meras, J. Chem. Phys. **105**, 6921 (1996).
[21] See, for example, T. Helgaker and P. Jørgensen, in *Methods in Computational Molecular Physics*, edited by S. Wilson and G. H. F. Diercksen (Plenum, New York, 1992), p. 353 ff.
[22] P. Pyykkö, Z. Naturforsch. Teil A **47**, 189 (1992).
[23] P. Pyykkö and A. J. Sadlej, Chem. Phys. Lett. **227**, 221 (1994).
[24] D. Sundholm, P. Pyykkö, and L. Laaksonen, Mol. Phys. **56**, 141 (1985).
[25] T. H. Dunning, J. Chem. Phys. **90**, 1007 (1989).
[26] R. A. Kendall, T. H. Dunning, and R. J. Harrison, J. Chem. Phys. **96**, 6796 (1992).
[27] D. E. Woon and T. H. Dunning, J. Chem. Phys. **98**, 1358 (1993).
[28] D. E. Woon and T. H. Dunning, J. Chem. Phys. **100**, 2975 (1994).
[29] D. E. Woon and T. H. Dunning, J. Chem. Phys. **103**, 4572 (1995). The core–valence basis sets were obtained from the Extensible Computational Chemistry Environment Basis Set Database, Version 1.0, as developed and distributed by the Molecular Science Computing Facility, Environmental and Molecular Sciences Laboratory which is a part of the Pacific Northwest Laboratory (PNL), P.O. Box 999, Richland, Washington 99352, USA, and funded by the U.S. Department of Energy. PNL is a multiprogram laboratory operated by Battelle Memorial Institute for the U.S. Department of Energy under Contract No. DE-AC06-76RLO 1830.
[30] P. Jørgensen and J. Simons, J. Chem. Phys. **79**, 334 (1983).
[31] L. Adamowicz, W. D. Laidig, and R. J. Bartlett, Int. J. Quantum Chem., Quantum Chem. Symp. **18**, 245 (1984).
[32] R. J. Bartlett, in *Geometrical Derivatives of Energy Surfaces and Molecular Properties*, edited by P. Jørgensen and J. Simons (Reidel, Dordrecht, 1986), p. 35 ff.
[33] T. Helgaker, H. Koch, A. Halkier, V. Bakken, O. Christiansen, and P. Jørgensen (unpublished).
[34] R. Krishnan, J. S. Binkley, R. Seeger, and J. A. Pople, J. Chem. Phys. **72**, 650 (1980).
[35] A. Schäfer, H. Horn, and R. Ahlrichs, J. Chem. Phys. **97**, 2571 (1992).
[36] A. Schäfer, C. Huber, and R. Ahlrichs, J. Chem. Phys. **100**, 5829 (1994).
[37] A. J. Sadlej, Col. Czech. Chem. Commun. **53**, 1995 (1988).
[38] P.-O. Widmark, P.-Å. Malmqvist, and B. O. Roos, Theor. Chim. Acta **77**, 291 (1990).
[39] P.-O. Widmark, B. J. Persson, and B. O. Roos, Theor. Chim. Acta **97**, 491 (1991).
[40] A. D. Buckingham, Adv. Chem. Phys. **12**, 107 (1967).
[41] J. Gauss and J. F. Stanton, J. Chem. Phys. **104**, 2574 (1996).
[42] K. Raghavachari, G. W. Trucks, J. A. Pople, and M. Head-Gordon, Chem. Phys. Lett. **157**, 479 (1989).
[43] G. E. Scuseria, T. J. Lee, R. J. Saykally, and H. F. Schaefer III, J. Chem. Phys. **84**, 5711 (1986).
[44] P. L. Cummins, G. B. Bacskay, N. S. Hush, and R. Ahlrichs, J. Chem. Phys. **86**, 6908 (1987).
[45] D. Cremer and M. Krüger, J. Phys. Chem. **96**, 3239 (1992).
[46] D. M. Bishop and S. M. Cybulski, J. Chem. Phys. **100**, 6628 (1994).
[47] F. Mata and M. C. Martin, J. Mol. Struct. **48**, 157 (1978).
[48] M. H. Coonan, I. A. Craven, M. R. Hesling, G. D. Ritchie, and M. A. Spackman, J. Phys. Chem. **96**, 7301 (1992).
[49] L. Serrano-Andrés, M. Merchn, I. Nebot-Gil, B. O. Roos, and M. Fülscher, J. Am. Chem. Soc. **115**, 6184 (1993).
[50] M. H. Palmer, I. C. Walker, C. C. Ballard, and M. F. Guest, Chem. Phys. **192**, 111 (1995).
[51] M. H. Sirvetz, J. Chem. Phys. **19**, 1609 (1951).
[52] J. Sheridan, in *Physical Methods in Heterocyclic Chemistry*, Vol. 6, edited by A. R. Katritzky (Academic, London 1974), p. 79.